Journal of Archaeological Science 37 (2010) 2705–2720

Contents lists available at ScienceDirect

Journal of Archaeological Science

journal homepage: http://www.elsevier.com/locate/jas

The use of SEM-EDS, PIXE and EDXRF for obsidian provenance studies in the Near East: a case study from Neolithic Çatalhöyük (central Anatolia)☆

Gérard Poupeau [a,b,*], François-Xavier Le Bourdonnec [a], Tristan Carter [c], Sarah Delerue [a], M. Steven Shackley [d], Jean-Alix Barrat [e], Stéphan Dubernet [a], Philippe Moretto [f], Thomas Calligaro [g], Marina Milić [h], Katsuji Kobayashi [i]

[a] Centre de Recherche de Physique Appliquée à l'Archéologie et Institut de Recherche sur les Archéomatériaux, UMR 5060, CNRS-Université Michel de Montaigne-Bordeaux 3, Esplanade des Antilles, 33607 Pessac, France
[b] UMR 5194 et Département de Préhistoire, CNRS-Muséum National d'Histoire Naturelle, Paris, France
[c] Department of Anthropology, McMaster University, Chester New Hall, 524, 1280 Main Street West, Hamilton, ON L8S 4L9, Canada
[d] Department of Anthropology/Archaeological XRF Laboratory, University of California, Berkeley, CA 94720-3710, USA
[e] CNRS/UBO, UMR 6538, Institut Universitaire Européen de la Mer, Place Copernic, 29280 Plouzané, France
[f] Université Bordeaux 1, CNRS/IN2P3, Centre d'Etudes Nucléaires de Bordeaux Gradignan, CENBG, Chemin du Solarium, BP120, 33175 Gradignan, France
[g] Centre de Recherche et de Restauration des Musées de France, UMR CNRS 171, 14 Quai François Mitterrand, 75001 Paris, France
[h] Institute of Archaeology, University College London, 31-34 Gordon Square, WC1H 0PY, United Kingdom
[i] School of Earth Sciences, The University of Melbourne, Melbourne, VIC 3010 Australia

ARTICLE INFO

Article history:
Received 10 February 2010
Received in revised form
30 May 2010
Accepted 8 June 2010

Keywords:
Obsidian sourcing
PIXE
SEM-EDS
Non-destructive analysis
Çatalhöyük
Anatolian Neolithic
East Göllü Dağ
Nenezi Dağ
Near East

ABSTRACT

In this paper we evaluate the relative analytical capabilities of SEM-EDS, PIXE and EDXRF for characterizing archaeologically significant Anatolian obsidians on the basis of their elemental compositions. The study involves 54 geological samples from various sources, together with an archaeological case study involving 100 artifacts from Neolithic Çatalhöyük (central Anatolia). With each technique the artifacts formed two compositional groups that correlated with the East Göllü Dağ and Nenezi Dağ sources. The non-destructive capabilities of these methods are emphasized (albeit with certain analytical limitations in the case of SEM-EDS), suggesting important new techniques for Near Eastern obsidian provenance studies.

1. Introduction

Obsidian was the primary raw material used by the inhabitants of Çatalhöyük (Konya Plain, central Anatolia) for the manufacture of their chipped stone tools throughout its Aceramic Neolithic – Early Chalcolithic occupation (c.7400–5500 cal BC, Cessford et al., 2005), despite the fact that the nearest sources are located ≥190 km to the northeast in the volcanic region of Cappadocia (Fig. 1). In 1999, as part of the renewed work at the site, a major program of obsidian characterization was initiated to investigate the long-term use of obsidian at Çatalhöyük. From the outset this work involved more than one laboratory and employed a range of analytical techniques (Table 1), i.e. our project is interested not only in the archaeological ramifications of our analyses, but also the collaborative development of innovative archaeometric approaches.

☆ This article is dedicated to the late Joseph Salomon, a former leading member of the AGLAE research group of the Centre de Recherche et de Restauration des Musées de France (Paris), with whom some of us initiated this obsidian provenance program fifteen years ago, Joseph, who passed away a few months ago, was a close collaborator and friend of several of the authors, and we feel both scientifically and humanly indebted to him.

* Corresponding author. Centre de Recherche de Physique Appliquée à l'Archéologie et Institut de Recherche sur les Archéomatériaux, UMR 5060, CNRS-Université Michel de Montaigne-Bordeaux 3, Esplanade des Antilles, 33607 Pessac, France.

E-mail addresses: gpoupeau@u-bordeaux3.fr, gpoupeau@mnhn.fr (G. Poupeau), Francois-Xavier.Le-Bourdonnec@u-bordeaux3.fr (F.-X. Le Bourdonnec), stringy@mcmaster.ca (T. Carter), shackley@berkeley.edu (M. Steven Shackley), barrat@univ-brest.fr (J.-A. Barrat), stephan.dubernet@u-bordeaux3.fr (S. Dubernet), moretto@cenbg.in2p3.fr (P. Moretto), thomas.calligaro@culture.fr (T. Calligaro), marina.milic.09@ucl.ac.uk (M. Milić), kats.koba@gmail.com (K. Kobayashi).

0305-4403/$ – see front matter © 2010 Published by Elsevier Ltd.
doi:10.1016/j.jas.2010.06.007

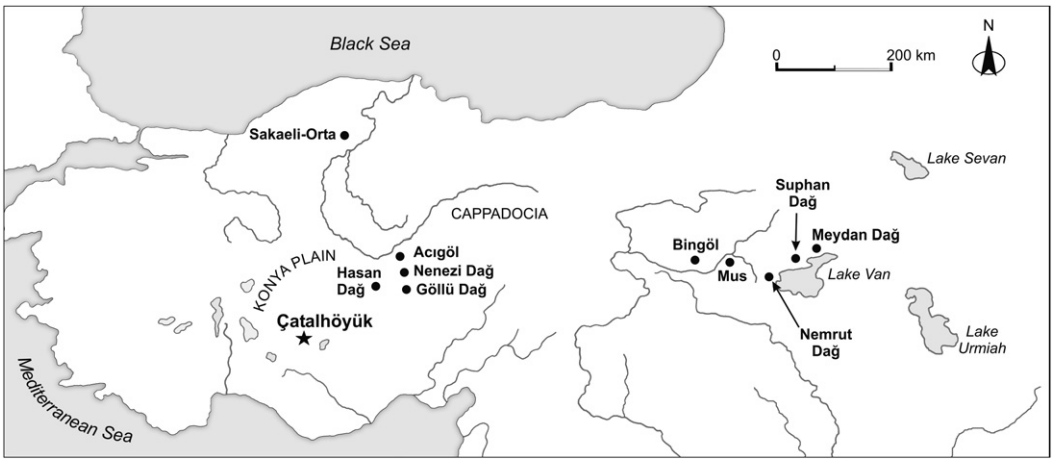

Fig. 1. Map of Anatolia showing the location of Çatalhöyük and the obsidian sources cited in the text.

Recent work at CRP2A (Bordeaux) has involved the investigation of two non-destructive analytical techniques that have received little, or no previous application in Near Eastern obsidian sourcing studies, namely scanning electron microscopy-energy dispersive spectroscopy (SEM-EDS) (Keller and Seifried, 1990; Delerue, 2007; Delerue and Poupeau, 2007) and particle induced x-ray emission (PIXE) (Abbès et al., 2003; Le Bourdonnec et al., 2005; Delerue, 2007; Carter et al., 2008). This paper focuses initially on the ability of these two methods to chemically discriminate some of the major Anatolian obsidian sources and to report new sourcing data using these approaches on 100 obsidian artifacts from Aceramic – Early Pottery Neolithic Çatalhöyük. Issues raised with some of the SEM-EDS data further led us to employ EDXRF, both as a means of analytical 'check and balance' and to integrate further another of the labs involved in our long-term international multi-technique/-researcher approach. The focus of this paper is therefore largely methodological, whereby the integrated *chaîne opératoire* analytical framework advocated by our team (Carter et al., 2006, 893–895), is detailed fully in a companion paper.

2. Provenance studies at Çatalhöyük

Çatalhöyük has long enjoyed a relationship with characterization studies, with four blades from the site included in the very first analysis of Near Eastern obsidians using OES in the 1960s (Renfrew et al., 1966), followed by the analysis of a further 11 artifacts over the next 35 years by OES, XRF and strontium isotope analyses (Gale, 1981; Keller and Seifried, 1990; Wright, 1969). Our new program of analyses has since characterized a further 527 samples, 100 of which form the archaeological basis of this paper (Table 1). While allowing for certain changes in source nomenclature over the past 40 years (Chataigner, 1998; Poidevin, 1998), the following general statements can be made concerning the history of obsidian use at Çatalhöyük (see Table 1 for all references): (1) throughout its history the two main sources exploited were East Göllü Dağ and Nenezi Dağ in southern Cappadocia (Fig. 1); (2) these obsidians were often consumed differently with regard to how they were worked and what was made from them, distinctions that cannot be explained through reference to mechanical properties alone; (3) the relative importance of these raw materials changed through time in terms of their proportion of the total obsidian assemblage; (4) during the later Early Pottery Neolithic (East Mound, Levels VI and upward) and Early Chalcolithic (West Mound) tiny quantities of obsidian were also procured from northern Cappadocian sources such as West Acıgöl and East Acıgöl ante caldera; (5) later Early Pottery Neolithic and Early Chalcolithic contexts have produced a handful of ready-made pressure-flaked blades made from eastern Anatolian obsidians, mainly the distinctive green peralkaline raw materials associated with the mountains of Bingöl and/or Nemrut Dağ, plus one made of a calc-alkaline product of Bingöl, sources located some 650–825 km distant, extending the western distribution of these obsidians by 300 km.

Table 1
Total number of Çatalhöyük obsidian artifacts sourced by our group and techniques used.

Laboratory	Artifacts[a]	Techniques	Publication
Grenoble (LGCA-CNRS)	100 (101)	ICP-AES; ICP-MS	Carter et al. (2005a, 2006)
Aberystwyth	35	LA-ICP-MS	Carter et al. (2005a, 2006)
Berkeley (2003)	42	EDXRF	Carter and Shackley (2007)
Bordeaux (CENBG-CNRS)	62 (62)	PIXE	This paper
Paris (C2RMF-CNRS) (2005)	10 (10)	PIXE	This paper
Bordeaux (IRAMAT-CNRS)	51	SEM-EDS	This paper
Berkeley (2008a)	34[b]	EDXRF	This paper
Berkeley (2007)	48 (53)	EDXRF	*in prep.*
Berkeley (2008b)	100	EDXRF	*in prep.*
Paris (C2RMF-CNRS) (2007a)	42 (46)	PIXE	Carter et al. (2008); *in prep.*
Paris (C2RMF-CNRS) (2007b)	15	PIXE	*in prep.*
Stanford	45	ICP-AES	*in prep.*
Total artifacts analyzed	557 (584)		

[a] The number in parentheses refer to the total number of analyses. Some artifacts have been measured more than once (by different labs).
[b] These artifacts and 17 others traited by PIXE were initially analyzed by SEM-EDS at IRAMAT-CNRS, they are not counted as new artifacts.

3. Sampling

3.1. Geological samples

In provenance studies, in order to ascertain source attributions, it is of great importance that the data from artifacts and geological samples are obtained under the same conditions. For this reason, geological samples were selected from sources of potential interest to be run alongside the archaeological artifacts using the same techniques. The obsidians under consideration come principally from Cappadocia, as these are the closest to Çatalhöyük and include raw materials already attested at the site by previous characterization studies (Appendix 1).

We deal first with the Göllü Dağ massif (Fig. 2) whose various obsidian outcrops have been geo-chemically grouped into two main compositional groups by Poidevin (1998, 115–121). The 'East Göllü Dağ' [hereafter EGD] type amalgamates the products of the East Kayırlı, Kömürcü and Sirça Deresi flows while the 'West Göllü Dağ' [hereafter WGD] type unites the obsidians of the Kayırlı-Village, North-Bozköy and Gösterli outcrops. The EGD 'source' was one of the major suppliers of obsidian throughout the prehistoric Near East (Carter et al., 2005a, 298–304; Chataigner, 1998, 285–292, Fig. 7b), with knapping workshops recognized atop various outcrops, not least that of the Aceramic Neolithic *atelier* of Kaletepe-Kömürcü (Balkan-Atli and Der Aprahamian, 1998; Binder and Balkan-Atli, 2001; Cauvin and Balkan-Atli, 1996 *inter alia*). Eleven source samples from Kömürcü and East-Kayırlı (EGD type) were selected for analysis, together with one sample from North-Bozköy (WGD type), even though the obsidian from latter flow is known to often have fissures and crystallization spherulites, i.e. of lesser quality for prehistoric knappers.

Three samples were also included from Nenezi Dağ, a volcano whose obsidians are often more compact and grainy than those of Kömürcü and East-Kayırlı (East Göllü Dağ), but are nonetheless known to have been used extensively by the inhabitants of Çatalhöyük and prehistoric communities throughout the Near East (Carter et al., 2005a, 298–304; Chataigner, 1998, 285, Fig. 5b). While knapping floors have been mapped on its western flanks, the actual geological outcrops are today obscured (Balkan-Atli et al., 1999, 135–136, Figs. 2 and 3).

In turn, eleven samples relating to the various outcrops of the Acıgöl region in northern Cappadocia were also analyzed (Fig. 3). Four samples come from the Bogazköy, Kartaltepe, Kocadağ and Tulucetepe flows that form part of the 'East Acıgöl *ante-caldera*' (EAAC) geo-chemical compositional group (Poidevin, 1998, 113). A further two samples came from Kocadağ, of the 'East Acıgöl *post-caldera*' type (EAPC), while the last five came from Körüdağ, Acıgöl crater and Güneydağ, flows that form part of the 'West Acıgöl' (WA) source (Poidevin, 1998, 113–114, Fig. 6).

In keeping with our desire to discriminate as many of the central Anatolian sources as possible, we also analyzed three geological samples from Hasan Dağ in western Cappadocia. While this is Çatalhöyük's closest source, there is no evidence to suggest that Hasan Dağ was ever exploited by this or any other community (*contra* the expectations of Mellaart (1967, 177)), its raw materials now appreciated to be poor-quality and difficult to access (Cauvin and Balkan-Atli, 1996, 252; Chataigner, 1998, 292–293). These

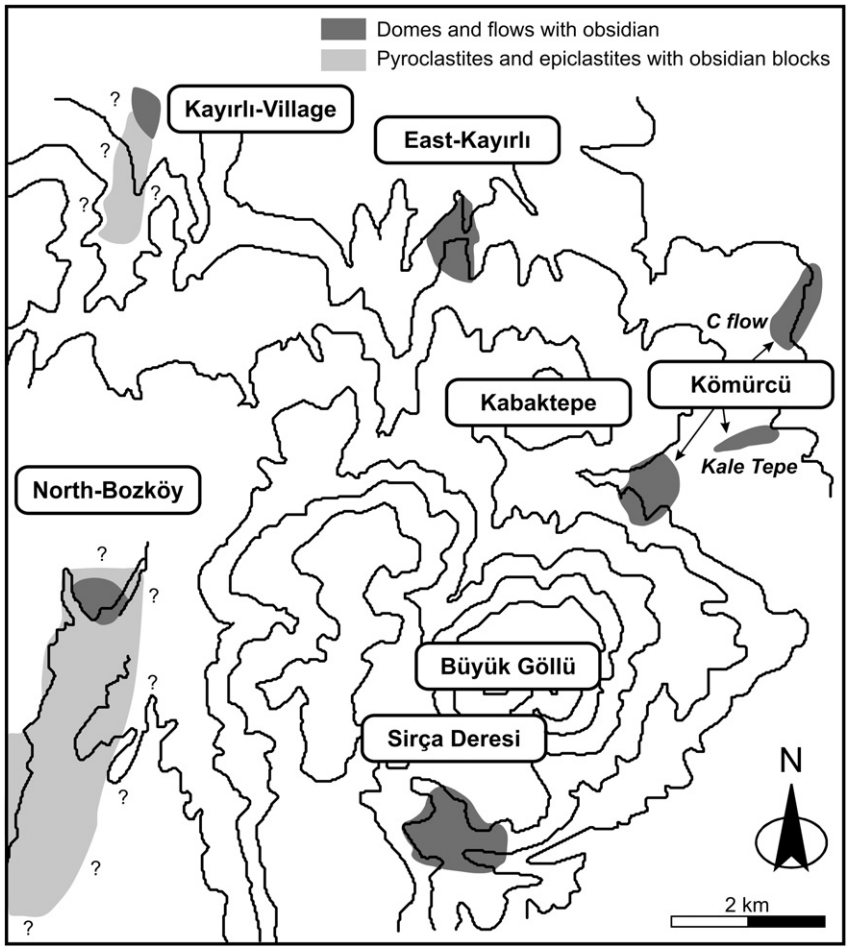

Fig. 2. Schematic map of the Göllü Dağ obsidian sources (modified from Poidevin, 1998).

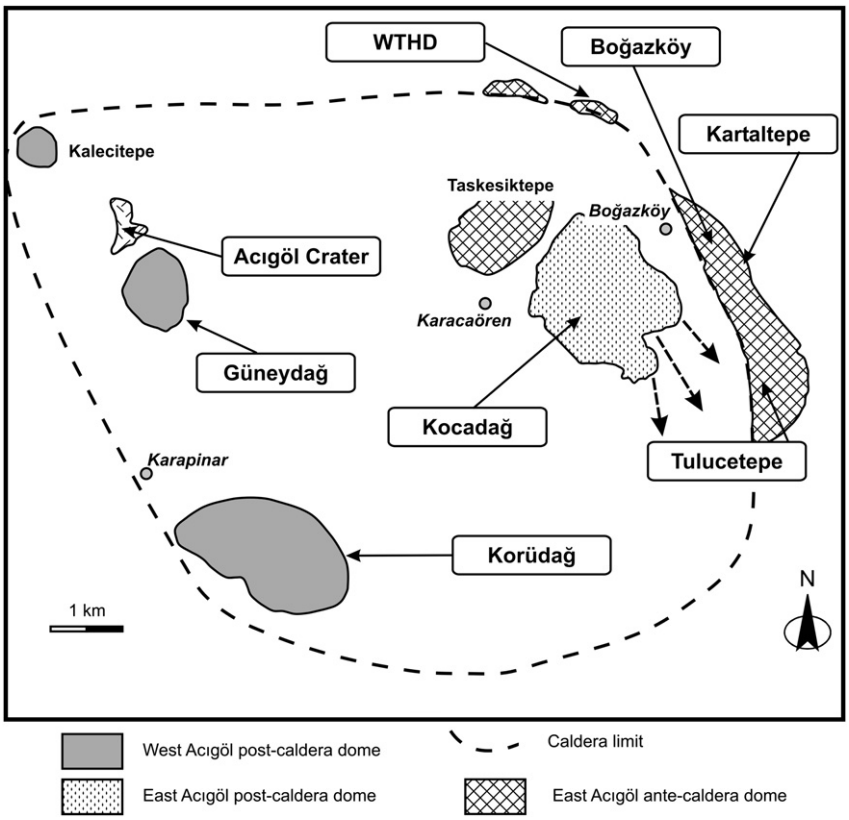

Fig. 3. Schematic map of the Acıgöl area obsidian sources (modified from Bigazzi et al., 1993 and Poidevin, 1998).

three samples came specifically from the 'Hasan Dağ' and 'Hasan Dağ-Kayırlı' locales as defined by Ercan et al. (1989).

Given that we now know that obsidians from southeastern Anatolia reached Çatalhöyük during the Early Ceramic Neolithic (Carter et al., 2008), we also felt it necessary to select obsidians from the major sources of the Bingöl area and Nemrut Dağ, together with samples from the nearby sources of Mus, Meydan Dağ and Süphan Dağ (Fig. 1).

Finally, we included one sample each from the Orta and Sakaeli sources in the Galatia region of northwest Anatolia, some 330 km from Çatalhöyük (Fig. 1), despite the fact that these obsidians have yet to be attested at the site, having seemingly only been used by local populations in the Neolithic (Chataigner, 1998, 275).

3.2. Archaeological samples

The 100 artifacts selected for analysis from Çatalhöyük came from various contexts on the East mound and the nearby/off-site Konya Basin Palaeoenvironments Project (KOPAL) trench, excavated during 1997–2004 (Hodder, 2007). Chronologically the material can be roughly subdivided into two data-sets: Aceramic Neolithic (OB200-OB239, OB245-OB249) and Early Pottery Neolithic (OB240-OB244, OB250-OB299); the assemblages from which these samples were selected are discussed fully elsewhere (Carter et al., 2005b). As a means of interrogating the relationship through time between raw material source and specific modes of exploitation (*chaînes opératoires*), the artifacts were chosen on the basis of a range of attributes: visual characteristics of raw material, technology, typology, date and context.

4. Analytical procedures

Methodologically this project's point of departure was to try and employ SEM-EDS and PIXE as analytical means of obsidian characterization and source discrimination in an Anatolian/Near Eastern context.

4.1. SEM-EDS

The SEM-EDS data were obtained at CRP2A with the Oxford Industries INCAx-sight energy dispersive spectrometer of a JEOL scanning electron microscope operating at 20 kV with an electron beam scanning a sample surface of 200–500 μm^2, with four to ten measurements per sample taken in different locations. In each analysis six elements, Na, Al, Si, K, Ca, and Fe were quantitatively determined; elements Ti, Mn and Mg were often below detection limits. Element contents were computed as 100% oxides. The geological samples were prepared as polished sections while the archaeological artifacts were analyzed non-destructively, i.e. with no surface preparation. The data were accumulated over a period of three years, with one source sample repeatedly analyzed in order to control the stability of the analytical system (P35-18B1 of the East-Kayirli source [EGD area]). The fifteen determinations taken over these 36 months do not reveal any drift with time (see also Le Bourdonnec et al., 2010). The smallest variations were found to be for Al, Si (less than one per cent), Na and K (less than six per cent). The largest dispersions were observed for Ca and Fe (albeit less than 9%). In the former case this is a reflection of the element's 'low' content with regard to our analytical system, while the latter can be explained with reference to intrinsic sample variations, as frequently found between multiple measurements of single samples and/or between aliquots of many obsidians.

4.2. PIXE

The PIXE analyses were performed in two laboratories (cf. Le Bourdonnec et al., 2005). At the *Centre d'Etudes Nucléaires de*

Table 2
Elemental compositions of Anatolian source samples as determined by SEM-EDS.

Area	Source	Sample	Surface	*n*	Na_2O	Al_2O_3	SiO_2	K_2O	CaO	Fe_2O_3	Type
Northwest Anatolia (Galatia)											
Orta		Or 4	PS	1*	3.54	12.60	77.01	5.23	0.77	0.78	Orta
Sakaeli		Sa 1	PS	1*	3.67	12.78	76.79	5.02	0.82	0.86	Orta
			FS	1	3.78	12.78	76.65	4.98	0.80	0.95	
Cappadocia											
Acıgöl	Acıgöl Crater	N8	PS	2**	3.74	11.62	78.97	4.46	0.40	0.80	WA
			FS	1	3.46	11.60	79.09	4.55	0.49	0.81	
		N9	PS	2**	3.81	11.63	78.95	4.43	0.41	0.78	WA
	Güneydağ	N10	PS	2**	3.75	11.76	78.81	4.44	0.41	0.80	WA
		N11	PS	2**	3.85	11.75	78.77	4.40	0.42	0.82	WA
	Körüdağ	N6	PS	2**	3.68	11.68	78.88	4.49	0.44	0.82	WA
			FS	1	3.89	11.89	78.60	4.43	0.40	0.78	
	Bogazköy	N7	PS	2**	3.60	12.25	77.86	4.68	0.72	0.87	EAAC
			FS	1	3.49	12.27	77.95	4.64	0.81	0.84	
	Kartaltepe	N2	PS	2**	3.59	12.19	77.80	4.68	0.79	0.95	EAAC
			FS	1	3.25	12.19	77.93	4.89	0.79	0.90	
	Tulucetepe	N3	PS	2**	3.62	12.17	77.99	4.65	0.72	0.85	EAAC
			FS	1	3.85	12.15	77.77	4.60	0.86	0.77	
	WTHD	N1	PS	2**	3.56	12.16	77.91	4.82	0.78	0.78	EAAC
			FS	1	3.65	12.29	77.86	4.76	0.77	0.68	
	Kocadağ	N4	PS	1*	3.97	12.83	76.41	4.39	0.96	1.42	EAPC
			FS	1	3.93	12.81	76.94	4.34	0.84	1.12	
		N5	PS	2**	3.89	12.76	76.54	4.39	0.97	1.40	EAPC
			FS	1	4.31	12.96	76.31	4.16	0.89	1.28	
Göllü Dağ	East Kayırlı	P35-18B1	PS	1	3.56	11.65	78.97	4.70	0.44	0.68	EGD
			FS	1	3.97	11.79	78.66	4.47	0.38	0.67	
		Kay E1	PS	1	3.51	11.64	79.05	4.68	0.42	0.69	EGD
			FS	2	3.47	12.02	78.75	4.58	0.45	0.75	
	Kömürçü	Kom 1	PS	1	3.53	11.68	78.98	4.64	0.42	0.72	EGD
			FS	1	3.80	11.80	78.70	4.65	0.41	0.64	
		Kom C1	PS	1	3.50	11.61	79.08	4.64	0.43	0.74	EGD
			FS	1	3.25	11.49	79.11	4.94	0.52	0.70	
		Kom C1b	FS	1	3.73	11.66	78.91	4.52	0.43	0.75	EGD
			PS	1	3.48	11.58	79.10	4.65	0.42	0.78	
			FS	1	3.59	11.53	79.16	4.57	0.49	0.66	
		Kom C4	FS	1	3.48	11.66	78.91	4.82	0.46	0.67	EGD
		Kom C5	PS	1	3.45	11.67	79.01	4.65	0.45	0.74	EGD
		KomC6	PS	1	3.47	11.64	79.22	4.53	0.45	0.70	EGD
			FS	1	3.59	11.57	78.91	4.78	0.41	0.69	
		Kom C11	PS	1	3.53	11.66	78.96	4.64	0.44	0.73	EGD
			FS	1	3.58	11.60	78.94	4.73	0.45	0.64	
		Kom C14	PS	1	3.43	11.62	79.02	4.79	0.46	0.69	EGD
			FS	1	3.63	11.70	78.98	4.62	0.45	0.62	
	North-Bozköy	N12	PS	5**	3.61	11.84	78.64	4.61	0.59	0.69	WGD
Hasan Dağ	Hasan Dağ	Hasan	PS	3**	3.71	12.12	78.72	4.25	0.60	0.55	Hasan
			FS	1	3.47	12.17	78.91	4.30	0.57	0.53	
	H. Dağ-Kayırlı	Has-Kay	PS	3**	3.73	12.49	77.29	4.62	0.86	0.95	Hasan
Nenezi Dag		P34.8	PS	2**	3.81	12.68	76.77	4.50	1.07	0.98	NNZD
			FS	3	3.56	12.53	76.93	4.75	1.12	1.02	
		NeW2	PS	2**	3.73	12.63	76.79	4.68	1.04	1.05	NNZD
			FS	1	3.73	12.70	76.83	4.73	1.00	0.97	
		NE 5	PS	2**	3.54	12.69	76.47	4.90	1.05	1.06	NNZD
			FS	1	4.02	12.89	76.63	4.49	1.01	0.90	
Southeastern Anatolia											
Bingöl	Ala Tepe	Ala Tepe 1	PS	3***	4.29	13.34	74.69	5.19	0.68	1.62	BB
			FS	1	3.85	13.25	74.50	5.81	0.78	1.73	
	Orta Duz	Orta D1	PS	1	4.61	9.66	76.35	4.85	0.17	4.22	BA/NMRD
			FS	1	4.83	9.87	76.67	4.59	<0.30	3.71	
		Orta D2	PS	2****	5.11	9.71	76.59	4.19	<0.20	4.12	BA/NMRD
			FS	3	4.59	9.53	76.30	4.96	0.19	4.28	
	Çavuslar	Çavuslar 1	PS	1	4.38	9.53	77.90	4.49	<0.20	3.56	BA/NMRD
			FS	1	4.22	9.68	78.21	4.46	<0.27	3.26	
		Çavuslar 2	PS	1	4.42	9.52	77.74	4.52	<0.20	3.56	BA/NMRD
			FS	1	3.88	9.60	78.27	4.58	<0.26	3.41	
		Çavuslar 4	PS	1	4.86	9.71	76.44	4.49	<0.20	4.16	BA/NMRD
			FS	1	5.07	9.64	76.12	4.70	0.21	4.06	
		Çavuslar 6	PS	1	4.73	9.15	77.25	4.36	<0.20	4.33	BA/NMRD
			FS	1	4.58	9.26	77.32	4.46	<0.41	4.08	
	Unspecified	Bingöl 1	PS	1	4.91	9.90	75.68	4.58	0.23	4.43	BA/NMRD
			FS	1	5.04	10.27	76.10	4.37	<0.22	3.89	
		Bingöl 2	PS	1	4.80	9.65	76.59	4.52	<0.20	4.23	BA/NMRD
			FS	1	4.57	9.72	76.94	4.52	<0.33	3.92	

(*continued on next page*)

Table 2 (*continued*)

Area	Source	Sample	Surface	*n*	Na_2O	Al_2O_3	SiO_2	K_2O	CaO	Fe_2O_3	Type
Lake Van	Meydan Dağ	Mey 1	PS	1*	4.37	12.09	77.36	4.49	0.38	1.29	MDD
			FS	2	4.61	12.09	77.24	4.35	0.42	1.27	
		Mey 4	PS	1*	4.35	12.16	77.36	4.44	0.48	1.20	MDD
			FS	2	4.55	12.38	77.04	4.32	0.43	1.27	
		D13	PS	1	4.19	12.03	77.30	4.74	0.38	1.29	MDD
			FS	1	4.10	12.02	77.84	4.42	0.36	1.22	
		D25	PS	1	4.34	12.06	77.30	4.50	0.45	1.34	MDD
			FS	1	4.21	12.15	77.48	4.42	0.43	1.31	
		D26	PS	1	4.41	12.13	77.25	4.43	0.39	1.35	MDD
			FS	1	4.41	12.25	77.45	4.38	0.37	1.15	
	Nemrut Dağ	Nem N1	PS	3**	4.55	10.32	77.35	4.58	<0.30	2.90	BA/NMRD
			FS	2	4.27	10.36	77.63	4.79	0.00	2.94	
		Nem N2	PS	1*	5.60	8.74	73.58	4.51	0.32	6.70	BA/NMRD
			FS	2	5.36	8.70	73.85	4.60	0.38	6.68	
		D2	PS	1	5.50	8.86	73.39	4.59	0.30	6.97	BA/NMRD
			FS	1	6.10	8.80	73.21	4.55	0.56	6.27	
		D4	PS	1	5.29	8.75	73.78	4.61	0.32	6.90	BA/NMRD
			FS	1	5.48	8.94	74.11	4.57	0.26	6.24	
		D21	PS	1*	5.64	8.88	74.06	3.46	0.32	7.14	BA/NMRD
			FS	1	5.55	8.92	73.70	4.84	0.35	6.28	
		D24	PS	1	5.50	8.76	73.56	4.63	0.22	6.88	BA/NMRD
			FS	1	4.29	8.19	73.18	3.83	2.07	7.92	
		D27	PS	1	5.62	8.59	73.44	4.58	0.27	7.04	BA/NMRD
			FS	1	5.21	8.45	73.32	4.63	0.35	7.47	
	Süphan Dağ	SUP 1	PS	1*	3.59	12.25	77.74	4.88	0.51	1.02	SPD
			FS	2	3.63	12.26	77.57	4.92	0.51	1.09	
		SUP 5	PS	1*	3.45	12.19	77.72	5.13	0.50	0.98	SPD
			FS	1	3.43	12.20	77.58	5.15	0.47	1.14	

PS, polished section, FS, fresh fracture surface; *n*, number of polished sections analyzed.
*Polished section measured twice; *n* polished sections, of which one was measured twice (**), five times (***) or six times (****). Polished section P35-18B1 was measured 15 times over a period of three years (see text).

Bordeaux-Gradignan (CENBG) the samples were analyzed on the 'Microbeam Line' of a 4 MV Van de Graaff accelerator (Llabador et al., 1990). In the vacuum sample chamber of this nuclear microprobe up to 15 samples could be introduced together, fixed on a rotating stage allowing us to make measurements on several points of their surface. A 3 MeV and 0.5 nA proton beam of 8 μm diameter was used on a scanning mode so that element contents were determined over a ~700 × 700 μm^2. At the *Centre de Recherche et de Restauration des Musées de France* (C2RMF, Paris), we used the extracted beam line of the AGLAE facility. The samples were fixed on an XYZ moving stage situated outside the accelerator, in front of the beam which exits through a 100 nm Si_3N_4 window. Up to 30 samples at once can be fixed on this stage. The distance between the accelerator exit and the sample under analysis is 2 mm. A proton beam of 3 MeV and 1 nA before accelerator exit, produced by a 2 MV Tandem Van de Graaff, reaches a diameter at sample surface of about 700 μm^2. During data acquisition the mean atomic number of the room ambient atmosphere is lowered in the volume of air between the accelerator exit, the sample and the XRF detector entries in order to limit absorption effects and X-ray spectra alterations (Calligaro et al., 1996, 2002). With regard to the non-destructive capabilities of these facilities, it should be noted that at CENBG only artifacts smaller than 3 cm long and 5 mm thick can be accepted, whereas at C2RMF with the external beam configuration of AGLAE there are no such size restrictions (cf. Calligaro et al., 2005). The source samples analyzed were the same as those previously analyzed by SEM-EDS; as before we focused on the polished sections with the exception of the Nenezi Dağ samples that were treated from fresh fractures on aliquots. Three Nemrut Dağ samples, NEM 3-1, 3-2 and 3-3 were only analyzed by PIXE (from polished sections).

In both systems, two Si(Li) detectors were used to simultaneously determine the contents of fifteen elements. The light elements Na, Al, Si, K, Ca, Ti, Mn and Fe signals were recorded by a 'low-energy' X-ray detector and the heavy elements Mn, Fe, Zn, Ga, Rb, Sr, Y, Zr and Nb by a 'high-energy' detector. Three measurements per sample were taken in different areas to account for possible local heterogeneities (phenocrysts, etc.). To insure data homogeneity, a reference sample was analyzed at least twice with each sample batch (obsidian ARC-URS [Le Bourdonnec, 2007]). Data was treated with the 2000 version of the GUPIX software (Maxwell et al., 1989; Campbell et al., 2000). Light (major) element contents for Na–Fe were calculated as 100% weight oxides. As the Fe signal is recorded in both detectors the content determined from the low energy detector spectrum was then used as an internal standard for the determination of trace elements contents. We have shown elsewhere that any bias in element content determinations between the CENBG and the C2RMF PIXE facilities, if present, were below counting statistics uncertainties (Le Bourdonnec et al., 2005). The only elements for which a content (oxide per cent or ppm) were computed are those that had a peak intensity in XRF spectra higher than 3σ above the detector mean background levels.

In order to critically appraise the quality of our PIXE data, and by extent its utility in Near Eastern obsidian characterization studies, we compared the results from 12 source samples with those generated from the exact same samples by Inductively Coupled Plasma – Mass Spectroscopy (ICP-MS) (see §6 below). The ICP-MS analyses were made at Brest University following the Tm-spiking procedure used by the CNRS group for over 10 years, a protocol that insures the internal consistency of all data obtained so far on Anatolian obsidians (Bellot-Gurlet, 1998; Abbès et al., 2003; Bellot-Gurlet et al., 2003; Bressy et al., 2005; Carter et al., 2006).

Finally, as a means of further interrogating our SEM-EDS data (see below) we turned to another of the project's long-term members, the UC Berkeley XRF laboratory (cf. Carter and Shackley, 2007). These analyses also provided us with means to critically review our inter-lab/multi-technique analytical approach.

4.3. EDXRF

Whole rock trace element analyses were performed in the Geoarchaeological XRF Laboratory, Department of Anthropology, University of California, Berkeley, using a ThermoScientific *Quant'X* energy dispersive x-ray fluorescence spectrometer. The spectrometer is equipped with a ultra-high flux peltier air cooled Rh x-ray target with a 125 micron beryllium (Be) window, an x-ray generator that operates from 4 to 50 kV/0.02 to 1.0 mA at 0.02 increments, using an IBM PC based microprocessor and WinTrace™ 4.1 reduction software. The spectrometer is equipped with a 2001 min^{-1} Edwards vacuum pump for the analysis of elements below titanium (Ti). Data is acquired with a pulse processor and analog to digital converter. This is a significant improvement in analytical speed and efficiency beyond the former Spectrace 5000 and *QuanX* analog systems (see Davis et al., 1998; Shackley, 2005).

For Ti–Nb, Pb, Th elements the mid-Zb condition is used operating the x-ray tube at 30 kV, using a 0.05 mm (medium) Pd primary beam filter in an air path at 200 s livetime to generate x-ray intensity Kα_1-line data for elements titanium (Ti), manganese (Mn), iron (as Fe^T), cobalt (Co), nickel (Ni), copper, (Cu), zinc, (Zn), gallium (Ga), rubidium (Rb), strontium (Sr), yttrium (Y), zirconium (Zr), niobium (Nb), lead (Pb), and thorium (Th). Not all these elements are reported since their values in many volcanic rocks is very low. Trace element intensities were converted to concentration estimates by employing a least-squares calibration line ratioed to the Compton scatter established for each element from the analysis of international rock standards certified by the National Institute of Standards and Technology (NIST), the US. Geological Survey (USGS), Canadian Centre for Mineral and Energy Technology, and the Centre de Recherches Pétrographiques et Géochimiques in France (Govindaraju, 1994). Line fitting is linear (XML) for all elements but Fe where a derivative fitting is used to improve the fit for iron and thus for all the other elements. When barium (Ba) is acquired, the Rh tube is operated at 50 kV and 1.0 mA in an air path at 200 s livetime to generate X-ray intensity Kα_1-line data, through a 0.630 mm Cu (thick) filter ratioed to the bremsstrahlung region (see Davis et al., 1998). A suite of 17 specific standards used for the best fit regression calibration for elements Ti–Nb, Pb, and Th, include G-2 (basalt), AGV-2 (andesite), GSP-2 (granodiorite), SY-2 (syenite), BHVO-2 (hawaiite), STM-1 (syenite), QLO-1 (quartz latite), RGM-1 (obsidian), W-2 (diabase), BIR-1 (basalt), SDC-1 (mica schist), BCR-2 (basalt), TLM-1 (tonalite), SCO-1 (shale), all US Geological Survey standards, BR-1 (basalt) from the Centre de Recherches Pétrographiques et Géochimiques in France, and JR-1 and JR-2 (obsidian) from the Geological Survey of Japan (Govindaraju, 1994).

The data from the WinTrace software were translated directly into Excel for Windows software for manipulation and on into SPSS for Windows for statistical analyses when necessary. In order to evaluate these quantitative determinations, machine data were compared to measurements of known standards during each run. RGM-1 is analyzed during each sample run for obsidian artifacts to check machine calibration.

5. Sourcing by SEM-EDS

The results of SEM-EDS analyses for 52 geological samples from 23 obsidian source-areas are presented in Table 2. The analyses were conducted either upon polished sections or freshly exposed surfaces. In most samples only one polished section was analyzed but in some cases up to five were prepared for a single sample. Several of these sections were analyzed twice or more, at intervals of several months. All repeats from single samples were in good agreement. Where a sample's elemental composition was determined more than once from the same polished section, we report only the average elemental contents (Table 2). When several polished sections were analyzed from the same sample, the data are averaged over these sections. Most elemental compositions were obtained by measurements on freshly exposed surfaces; in these cases measurements were made only once. In general the agreement between the element contents measured on polished sections and freshly exposed surfaces is excellent (Table 2). Rare exceptions are found only for Na, where they exceed only 11% (sample N5 of Koçadag, Göllü Dağ area) to 21% (N4, Koçadağ) respectively. The main differences between source chemistry relate to their Al, Si, Ca and Fe contents.

The 51 Çatalhöyük artifacts tentatively sourced using SEM-EDS were easily separated into two groups, Ca–Fe 'poor' and 'rich', comprising 43 and eight artifacts respectively (Table 3). While

Table 3
Elemental compositions of Çatalhöyük obsidian artifacts as determined non-destructively by SEM-EDS. The samples are ordered by increasing Na_2O content.

Sample	Na_2O[a]	Al_2O_3	SiO_2	K_2O	CaO	Fe_2O_3
Ca–Fe poor artifacts						
OB220	2.38	11.28	79.08	6.06	0.43	0.77
OB229	2.48	11.35	79.07	5.76	0.53	0.77
OB230	2.51	11.69	78.46	6.23	0.45	0.66
OB241	2.56	11.53	79.07	5.59	0.52	0.72
OB224	2.68	11.39	79.27	5.41	0.61	0.64
OB225	2.74	11.67	78.99	5.43	0.45	0.72
OB200	2.85	11.44	79.03	5.37	0.55	0.71
OB210	2.89	11.65	79.17	5.20	0.45	0.60
OB266	2.89	11.74	78.96	5.37	0.42	0.61
OB207	2.93	11.76	78.85	5.33	0.52	0.61
OB273	2.94	11.51	78.80	5.38	0.50	0.82
OB240	2.97	11.69	78.79	5.32	0.52	0.70
OB270	2.97	11.77	78.88	5.22	0.46	0.69
OB232	3.01	11.78	78.90	5.25	0.45	0.61
OB208	3.02	11.57	78.85	5.27	0.49	0.79
OB234	3.03	12.17	78.56	5.27	0.46	0.51
OB264	3.03	11.72	78.85	5.30	0.44	0.62
OB299	3.03	11.76	78.78	5.30	0.48	0.65
OB227	3.06	11.67	78.77	5.33	0.45	0.73
OB252	3.06	11.59	78.77	5.47	0.46	0.64
OB218	3.07	11.52	78.89	5.35	0.52	0.65
OB216	3.18	11.58	78.96	5.05	0.54	0.71
OB221	3.22	11.55	78.99	4.96	0.47	0.76
OB219	3.25	11.93	78.84	5.02	0.37	0.60
OB261	3.26	11.64	78.76	5.16	0.45	0.73
OB233	3.27	11.80	78.85	5.09	0.54	0.44
OB296	3.27	12.13	79.03	4.83	0.32	0.42
OB236	3.35	11.71	79.18	4.80	0.42	0.55
OB247	3.39	11.54	79.04	4.81	0.49	0.73
OB244	3.45	11.95	78.87	4.78	0.38	0.57
OB267	3.47	11.66	78.43	5.08	0.53	0.75
OB246	3.48	11.74	79.04	4.71	0.37	0.66
OB202	3.49	11.67	79.06	4.63	0.46	0.65
OB265	3.55	11.92	79.22	4.48	0.37	0.46
OB214	3.73	12.17	78.69	4.41	0.44	0.56
OB231	3.73	12.10	78.94	4.29	0.36	0.53
OB203	3.76	12.04	78.25	5.07	0.37	0.51
OB204	3.77	11.78	78.87	4.52	0.51	0.55
OB211	3.79	12.01	78.92	4.35	0.45	0.47
OB260	3.86	12.10	78.81	4.44	0.32	0.47
OB262	4.05	12.04	78.81	4.13	0.39	0.58
OB245	4.06	12.19	78.64	4.38	0.33	0.40
OB248	4.14	12.03	78.59	4.27	0.50	0.46
Ca–Fe rich artifacts						
OB278	2.89	12.71	76.78	5.33	1.20	1.09
OB256	2.96	12.61	76.76	5.28	1.14	1.14
OB213	3.61	12.84	76.71	4.79	1.04	0.94
OB272	3.68	12.68	77.04	4.67	0.99	0.90
OB212	3.82	12.77	76.72	4.62	0.98	0.99
OB215	3.87	13.00	76.58	4.37	1.21	0.93
OB277	3.94	12.96	76.61	4.52	1.06	0.86
OB228	4.03	12.94	76.51	4.59	0.97	0.95

[a] Element contents in weight per cent oxides.

previous reports of the sodium contents of Anatolian obsidians – as expressed in oxides – have varied from 3.4% to more than 4% (Poidevin, 1998), our SEM-EDS analyses produced anomalously low values down to 2.89% and 2.38% in the high and low Ca–Fe groups respectively (Table 3). Moreover, as Na contents decrease, one observes a linear anti-correlation with K contents, a slight progressive decrease in Al, a subtle increase in Si, more important and irregular values for Fe and small erratic variations in Ca. This is attributed to the alteration of the obsidian's chemical composition that results from the hydration of a superficial layer that accumulates during the artifacts' post-use burial in soil. Element content profiling by secondary ion mass spectrometry has shown that in the first micron or so below the surface of an hydrated obsidian, the Na and K contents are considerably enhanced and lowered respectively, while those of Ca and Fe are variably affected (cf. Adams, 1984; Patel et al., 1998, p. 1049; Anowitz et al., 1999, Fig. 3). In order to test this hypothesis we determined the SEM-EDS composition on a polished (internal) surface of five artifacts with various Na contents, followed by a series of measurements on the same artifacts' external surfaces (Table 4). While on the external surfaces the analyses were made on only three to five different locations against 10 for the internal surface the standard deviation about the mean values are in general quite similar. However, one observes that the compositions determined from the (modern) internal surfaces are significantly different from those determined from the (archaeological) external surfaces. In particular their Na contents are now in the usual obsidian range, which supports the surface alteration hypothesis for the data obtained in non-destructive analyses. The 'internal surface' compositions of these five artifacts are in fact very similar to each other and appear now to be in the range to be expected for East Göllü Dağ obsidians (Fig. 4). Thus the data obtained on these artifacts raises the question of the utility of non-destructive SEM-EDS artifact analysis in provenance studies.

In the high Ca–Fe artifacts groups, only two artifacts (OB 256 and 278) present a visibly affected Na content accompanied by minor effects on K and Fe (Table 3). When plotted in a Fe *vs.* Ca diagram these artifacts are located in the vicinity of the Nenezi Dağ

Table 4
Comparison between the SEM-EDS compositions of five artifacts as determined on 'archaeological' and polished surfaces respectively.

Sample	Surface*	*n*		Na_2O	Al_2O_3	SiO_2	K_2O	CaO	Fe_2O_3
OB200	AS	5	average	2.85	11.44	79.03	5.37	0.55	0.71
			st. dev.	*0.10*	*0.14*	*0.24*	*0.08*	*0.05*	*0.05*
	PS	10	average	3.54	11.71	79.01	4.58	0.43	0.73
			st. dev.	*0.10*	*0.17*	*0.21*	*0.15*	*0.07*	*0.17*
OB208	AS	5	average	3.02	11.57	78.85	5.27	0.49	0.79
			st. dev.	*0.14*	*0.14*	*0.25*	*0.12*	*0.05*	*0.14*
	PS	10	average	3.56	11.58	79.09	4.63	0.45	0.68
			st. dev.	*0.08*	*0.19*	*0.21*	*0.09*	*0.06*	*0.08*
0B220	AS	3	average	2.38	11.28	79.08	6.06	0.43	0.77
			st. dev.	*0.24*	*0.14*	*0.58*	*0.12*	*0.12*	*0.33*
	PS	9	average	3.50	11.61	79.01	4.69	0.43	0.75
			st. dev.	*0.11*	*0.17*	*0.19*	*0.09*	*0.05*	*0.16*
OB233	AS	5	average	3.27	11.80	78.85	5.09	0.54	0.44
			st. dev.	*0.17*	*0.14*	*0.14*	*0.12*	*0.07*	*0.04*
	PS	10	average	3.54	11.74	78.94	4.61	0.45	0.73
			st. dev.	*0.11*	*0.14*	*0.25*	*0.09*	*0.06*	*0.11*
OB296	AS	5	average	3.27	12.13	79.03	4.83	0.32	0.42
			st. dev.	*0.10*	*0.08*	*0.18*	*0.11*	*0.06*	*0.04*
	PS	10	average	3.55	11.68	78.86	4.69	0.45	0.77
			st. dev.	*0.08*	*0.14*	*0.13*	*0.07*	*0.07*	*0.08*

n, number of spot measurements per sample; element contents in weight per cent oxides.
* AS, archaeological surface; PS, polished section.

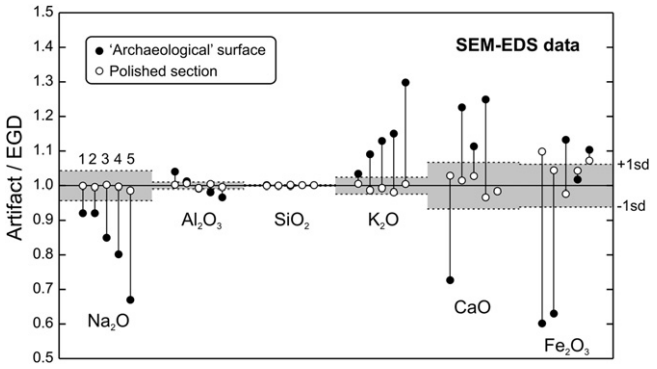

Fig. 4. Comparison for five Çatalhöyük artifacts between the normalized SEM-EDS elemental compositions determined non-destructively on 'archaeological' and on polished surfaces respectively. The norm is taken as the average composition of East Göllü Dağ obsidians calculated from the 10 samples of Table 2.

obsidians and not very far from those of the Galatia, Hasan Dağ and the ante- and post-Acıgöl sources (Fig. 5). However, the Galatia (Orta and Sakaeli) obsidians, which are claimed to have a very homogeneous composition (Poidevin, 1998), systematically present Ca and Fe contents lower than in Nenezi Dağ obsidians (Keller and Seifried, 1990), as also observed in Table 2 and PIXE analyses (below Table 5). With regard to the East Acıgöl post-caldera obsidians (Kocadağ), their Fe contents are known to be higher than in Nenezi Dağ obsidians (Keller and Seifried, 1990), as also seen here by SEM-EDS (Table 2) and PIXE analyses (Table 5). Similarly, the Ca contents of the East Acıgöl ante-caldera obsidians are lower than in those of the Nenezi Dağ (Keller and Seifried, 1990 and here, Tables 3 and 5). Thus on purely analytical grounds a Galatia or Acıgöl origin are unlikely for the raw material of the high Ca–Fe artifacts group. It may also be noted that the Galatian sources of Orta and Sakaeli were apparently exploited only locally (Chabot et al., 2001; Chataigner, 1998, 275), while these Acıgöl sources were only rarely used (Chataigner, 1998). With Hasan Dağ obsidians not seeming to have been used by ancient people (Chataigner, 1998), one could rather safely assume that like the other Ca–Fe rich Çatalhöyük obsidians previously sourced by ICP-AES and ICP-MS (Carter et al., 2006), those analyzed here by SEM-EDS also come from Nenezi Dağ (see also below).

The situation is not so clear-cut with the low Ca–Fe group of artifacts. In a Ca–Fe binary plot of the Fig. 5 type they would be

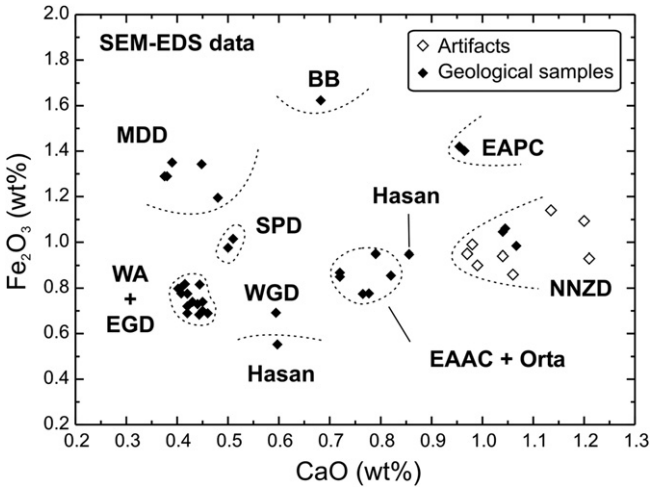

Fig. 5. Comparison between the Ca and Fe contents in the Çatalhöyük high Ca–Fe group of artifacts and in obsidians from potential sources as determined by SEM-EDS. Source abbreviations as in Table 2.

Table 5
Elemental compositions of Anatolian geological obsidians as determined by PIXE, ICP-AES, ICP-MS and EDXRF.

Area	Source	Type	Sample	Method/Lab	Na_2O	Al_2O_3	SiO_2	K_2O	CaO	TiO_2	MnO	Fe_2O_3	Zn	Ga	Rb	Sr	Y	Zr	Nb	Ba	Th
Northwestern Anatolia																					
Orta		Orta	Or4	PIXE/C2RMF	4.1	13.5	75.7	4.8	0.72	0.119	0.054	0.83	40	15	189	120	20	135			33
				ICP-MS						0.124	0.057		41.2	14.7	164	110.2	12.5	134.0	26.9	492	28.0
				EDXRF							0.060				176	114	16	140	26	639	20
Sakaeli		Orta	Sa 1	PIXE/C2RMF	4.1	13.6	75.6	4.6	0.77	0.194	0.059	0.90	40	17	188	151	17	150			37
				ICP-MS						0.131	0.058		41.3	14.7	160	126.9	12.4	143.2	26.7	538	27.1
				EDXRF							0.050				165	121	11	148	25	636	25
Cappadocia																					
Acıgöl	Acıgöl crater	WA	N8	EDXRF							0.060		44	18	267	3	42	87	30	29	35
			N8	PIXE/C2RMF	4.1	12.8	77.5	4.0	0.39	0.023	0.068	0.74	31	18	266	< 2	35	79	35		
	Kocadağ	AEPC	N4	PIXE/C2RMF	4.2	13.9	74.5	3.9	0.93	0.137	0.064	1.65	45	17	165	100	30	185	23		
	WTHD	AEAC	N1	PIXE/C2RMF	3.8	13.3	76.3	4.3	0.72	0.073	0.050	0.97	33	15	180	63	22	110	16		
Göllü Dağ	East Kayırlı	EGD	P35-18B1	PIXE/CENBG *	3.9	12.8	79.3	4.4	0.42	0.050	0.060	0.75	19	16	201	12		66			
				PIXE/C2RMF **	4.3	13.1	76.7	4.1	0.41	0.050	0.060	0.75	20	15	191	9		68			
				PIXE:C2RMF	4.1	12.4	77.7	4.2	0.43	0.053	0.064	0.89	22	18	236	11	27	90			
			P35-18B1	ICP-MS						0.051	0.061		23.6	14.0	186	9.0	22.2	70.0	22.4	96	21.4
		EGD	Kay E1	ICP-MS						0.054	0.063		22.8	14.2	182	9.9	22.1	72.6	23.6	114	22.0
	Kömürçü	EGD	Kom-1	EDXRF							0.056		40	17	194	17	23	86	26	222	26
				ICP-MS						0.040	0.059		22.3	13.7	173	11.9	20.7	71.2	22.6	154	21.3
		EGD	Kom C1	PIXE/CENBG	3.8	12.8	78.2	4.3	0.43	0.055	0.051	0.62	22	17	216	11	26	73	33		
				ICP-MS						0.031	0.061		23.0	14.0	186	8.9	22.3	71.2	22.9	97	21.4
		EGD	Kom C1b	PIXE/CENBG	3.8	12.8	78.1	4.2	0.41	0.055	0.056	0.65	20	15	185		<17	56			
				ICP-MS						0.052	0.059		24.9	13.2	179	8.8	21.7	68.7	18.9	101	21.2
		EGD	Kom C3	ICP-MS						0.051	0.060		21.3	13.7	178	9.2	21.6	69.7	23.7	101	21.2
		EGD	Kom C4	PIXE/CENBG	3.9	12.8	77.9	4.2	0.41	0.060	0.057	0.68	21	14	170	8	29	75	36		
		EGD	Kom C5	PIXE/CENBG	3.9	12.7	77.9	4.3	0.42	0.050	0.059	0.67	22	12	165	17	21	76	20		
		EGD	Kom C11	PIXE/CENBG	3.8	12.7	78.1	4.3	0.42	0.060	0.058	0.69	20	13	168	14	27	79	37		
		EGD	Kom C14	PIXE/CENBG	3.9	12.6	78.0	4.3	0.43	0.054	0.051	0.64	20	12	187	12	26	84	32		
		EGD	Kom C15	PIXE/CENBG	3.3	12.8	77.6	5.0	0.42	0.058	0.051	0.65	17	17	191	14	<15	65	32		
	Sirça Deresi	EGD	SD 1	PIXE/C2RMF	3.8	12.6	78.0	4.3	0.41	0.056	0.064	0.72	18	15	211	8	20	74	26		
		EGD	SD2	PIXE/C2RMF	3.9	12.7	78.0	4.3	0.41	0.049	0.066	0.73	18	15	205	11	22	65	27		
	North-Bozköy	WGD	N12	PIXE/C2RMF	3.9	12.9	77.2	4.2	0.57	0.073	0.056	0.70	24	14	165	40	13	74	21		
Hasan Dağ		Hasan	Hasan	PIXE/C2RMF	4.1	13.3	77.1	3.6	0.58	0.092	0.051	0.58	19	14	122	74	16	49	16		
Nenezi Dağ		NNZD	P34.8	PIXE/CENBG	4.3	13.7	74.8	4.1	0.99	0.121	0.071	1.24	48	17	191	118		125			
				ICP-MS						0.113	0.064		42.6	14.3	154	92.9	19.2	136.7	19.5	539	6.9
		NNZD	Ne W2	PIXE/CENBG	3.8	13.1	76.7	4.3	1.18	0.130	0.080	1.27	40	18	182	115		154			
				ICP-MS						0.119	0.066		46.9	14.7	160	96.7	19.8	139.1	18.6	549	7.0
		NNZD	NE 5	PIXE/CENBG	4.0	13.6	75.0	4.3	1.10	0.124	0.083	1.32	42	21	179	129	25	179	23		
				ICP-MS						0.110	0.063		42.1	13.8	158	90.0	20.5	138.5	20.5	542	7.3
Southeastern Anatolia																					
Bingöl	Ala Tepe	BB	Al Te 1	PIXE/CENBG *	4.5	14.3	71.9	4.7	0.71	0.200	0.040	1.79	44	18	221	63		282			
				PIXE/C2RMF **	4.8	14.9	72.3	4.9	0.68	0.197	0.039	1.76	49	21	219	41		326			
	Orta Duz	BA	Orta D 2	PIXE/CENBG *	6.3	10.4	75.3	3.0	0.15	0.180	0.060	4.22	199	28	225	< 10		1102			
				PIXE/C2RMF **	6.3	11.1	74.3	3.2	0.22	0.181	0.074	4.14	210	39	205	< 12		1324			
		BA	BIN 9-1	PIXE/C2RMF	5.3	10.6	75.2	4.1	0.19	0.198	0.071	4.04	198	31	236	< 6	125	1184	66		

(*continued on next page*)

Table 5 (*continued*)

Area	Source	Type	Sample	Method/Lab	Na_2O	Al_2O_3	SiO_2	K_2O	CaO	TiO_2	MnO	Fe_2O_3	Zn	Ga	Rb	Sr	Y	Zr	Nb	Ba	Th
Lake Van	Meydan Dağ	MDD	ME 6-1	PIXE/C2RMF	4.7	13.2	76.3	4.1	0.39	0.077	0.065	1.30	68	18	206	21	50	261	37		
		MDD	ME 7-1	PIXE/C2RMF	4.8	13.1	76.3	4.1	0.38	0.073	0.064	1.28	69	19	206	18	48	262	37		
		MDD	Mey 1	ICP-MS						0.070	0.068		85.6	19.4	211	15.2	62.7	303.9	26.9	57	8.7
		MDD	Mey 4	ICP-MS						0.080	0.065		82.2	18.2	197	18.6	56.7	280.4	24.6	67	7.8
	Mus	MUS	D20	PIXE/C2RMF	4.9	13.6	75.2	4.0	0.37	0.045	0.051	1.15	98	28	184	4	60	190	83		
		MUS	Mus Ziy	PIXE/C2RMF	5.0	13.5	75.0	3.9	0.38	0.046	0.053	1.24	103	29	191	< 2	60	200	87		
	Nemrut Dağ	NMRT	Nem N1	PIXE/CENBG	4.6	11.3	77.5	4.2	0.23	0.150	0.060	2.81	161	26	245	< 6		1323			
				ICP-MS						0.140	0.053		183.4	28.2	191	0.1	127.4	1234	57.0	1	24.7
		NMRT	Nem N2	ICP-MS						0.212	0.107		170.1	18.4	147	0.2	94.9	982.0	52.8	2	21.3
		NMRT	NEM 3-1	PIXE/C2RMF	6.0	9.6	72.6	4.1	0.30	0.336	0.167	6.32	242	28	252	< 10	162	1382	95		
		NMRT	NEM 3-2	PIXE/C2RMF	6.0	9.6	72.4	4.1	0.29	0.349	0.167	6.41	241	27	245	< 10	151	1346	100		
		NMRT	NEM 3-3	PIXE/C2RMF	5.6	11.9	73.8	4.2	0.28	0.212	0.081	5.88	171	29	224	< 5	113	1130	79		
	Suphan Dağ	SPD	Sup 1	ICP-MS						0.07	0.034		44.5	17.4	162	15.5	35.6	102.5	9.2	517	18.8
		SPD	SUP 5	PIXE/CENBG	3.7	13.2	76.3	4.6	0.47	0.067	0.034	1.41	36	17	156	16	26	90	10		
				ICP-MS						0.020	0.032		35.4	16.5	154	14.3	33.6	95.4	9.3	478	16.9
		SPD	SU 5-1	PIXE/C2RMF	3.8	13.3	76.7	4.5	0.47	0.062	0.030	1.12	31	18	152	17	22	89	11		

Contents in oxides are in weight per cent and contents in trace elements in μg/g (ppm); PIXE data were obtained from polished sections (sample reference numbers underlined) or fresh fractures (other samples); ICP-AES were used for the determination of major and minor elements Na to Fe and ICP-MS for trace elements Zn to Th.
*Delerue (2007); **Le Bourdonnec et al. (2005).

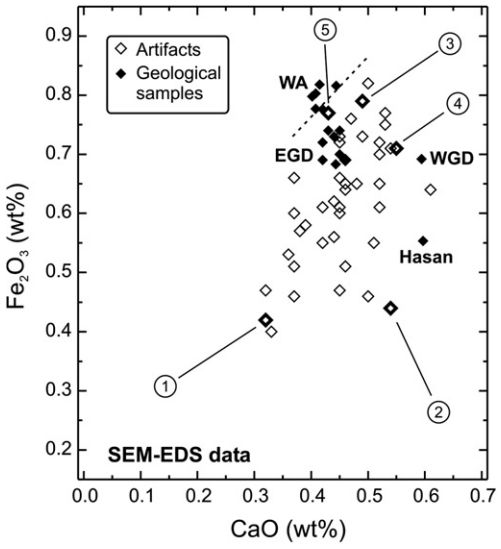

Fig. 6. Comparison between the Ca and Fe contents in the Çatalhöyük low Ca–Fe artifacts group and in obsidians from potential sources as determined by SEM-EDS. Source abbreviations as in Table 2. Samples numbered 1 to 5 are the same as in Fig. 4.

located in the lower left corner near to several source compositions. In an enlarged plot of this area the Çatalhöyük artifacts appear rather dispersed around the obsidians of East Göllü Dağ and also in the immediate vicinity of those from Hasan Dağ, West Acıgöl and West Göllü Dağ (Fig. 6). It has to be remembered however that all the artifact compositions reported were obtained on external surfaces. The artifacts numbered 1–5 in Fig. 6 are those that were selected for the determination of an internal surface composition (Table 4). They were intentionally chosen for their extreme contents in Ca and/or Fe contents. The fact their 'internal surface' composition is in close agreement with that of EGD and WA obsidians suggests, but do not prove, that this might also be the case for the other low Ca–Fe artifacts. If this was the case, and considering that WGD and Hasan Dağ obsidians are extremely rare/absent from Neolithic assemblages, we would thus suggest that low Ca–Fe obsidians determined by SEM-EDS from Çatalhöyük have an East Göllü Dağ or West Acigöl source, while also keeping in mind that only one artifact made from the latter raw material has thus far been attested at Çatalhöyük out of the aforementioned 527 samples run (Table 1). Simply stated, while we cannot be absolutely certain

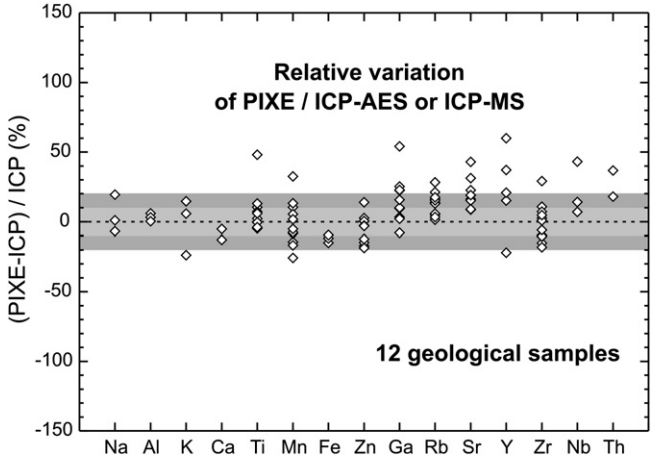

Fig. 7. Comparison between the elemental compositions determined by PIXE and ICP on aliquots from Anatolian obsidians. The contents of Na to Fe were determined by ICP-AES and for the heavier elements by ICP-MS.

Table 6
Elemental compositions of Çatalhöyük obsidian artifacts as determined by PIXE. The samples are ordered by increasing Na_2O content.

Sample	Facility	Na_2O	Al_2O_3	SiO_2	K_2O	CaO	TiO_2	MnO	Fe_2O_3	Zn	Ga	Rb	Sr	Y	Zr	Nb
Ca–Fe and Sr–Zr poor artifacts																
OB220	C2RMF	1.9	13.1	79.1	4.6	0.46	0.053	0.059	0.76	20	15	197	16	23	74	22
	CENBG	3.1	12.6	78.2	4.7	0.44	0.056	0.062	0.73	19	13	185	19	17	66	22
OB233	C2RMF	1.9	13.0	79.1	4.6	0.46	0.069	0.063	0.74	20	15	202	14	24	69	24
	CENBG	3.1	12.7	78.2	4.6	0.47	0.048	0.064	0.73	21	12	199	12	–	72	–
OB296	C2RMF	1.9	12.9	79.1	4.6	0.45	0.067	0.065	0.85	23	17	205	19	26	78	28
	CENBG	3.2	12.8	78.2	4.5	0.48	0.064	0.057	0.66	21	12	177	20	–	67	21
OB200	C2RMF	2.0	13.0	79.1	4.6	0.46	0.054	0.064	0.74	20	15	218	17	25	73	29
OB229	C2RMF	2.0	13.0	79.2	4.5	0.46	0.057	0.062	0.78	20	16	201	13	19	66	26
OB221	C2RMF	2.2	13.0	79.0	4.5	0.47	0.063	0.061	0.81	21	15	192	20	20	73	25
OB289	CENBG	2.7	12.5	79.0	4.8	0.51	0.061	0.085	0.96	30	17	264	11	–	98	–
OB268	CENBG	2.8	13.0	78.5	5.1	0.47	0.074	0.062	0.85	24	16	210	20	–	79	–
OB226	CENBG	2.9	12.5	78.7	4.9	0.52	0.090	0.071	0.94	26	15	212	17	–	80	–
OB299	CENBG	2.9	12.7	77.8	4.7	0.49	0.071	0.081	0.89	28	16	231	14	–	76	26
OB230	CENBG	3.0	12.7	78.1	4.7	0.46	0.050	0.069	0.69	21	14	184	9	–	84	–
OB242	CENBG	3.0	12.3	79.0	4.9	0.50	0.093	0.064	0.86	26	16	230	15	–	84	–
OB253	CENBG	3.0	12.7	78.8	4.6	0.45	0.077	0.065	0.84	27	17	216	15	–	79	–
OB266	CENBG	3.0	12.8	78.0	4.7	0.44	0.062	0.067	0.75	18	17	212	12	–	80	20
OB203	CENBG	3.1	12.8	78.0	4.5	0.47	0.060	0.064	0.72	21	17	205	10	–	–	21
OB208	C2RMF	3.1	12.7	78.4	4.5	0.44	0.058	0.065	0.80	22	17	229	14	27	82	27
OB234	CENBG	3.1	12.8	78.0	4.6	0.47	0.058	0.057	0.73	23	15	189	12	–	–	20
OB254	CENBG	3.1	12.5	79.1	4.9	0.49	0.075	0.066	0.84	23	16	209	20	–	74	–
OB255	CENBG	3.1	12.7	78.8	4.8	0.48	0.072	0.066	0.87	27	19	236	18	–	92	–
OB205	CENBG	3.2	12.6	77.7	5.0	0.50	0.072	0.082	1.10	28	22	270	17	–	95	–
OB206	CENBG	3.2	12.7	79.0	4.7	0.46	0.070	0.065	0.87	25	15	224	19	–	79	–
OB209	CENBG	3.2	12.8	79.3	4.7	0.46	0.061	0.057	0.78	22	16	204	17	–	84	–
OB257	CENBG	3.2	12.7	79.1	4.7	0.50	0.076	0.065	0.83	24	14	215	24	–	68	–
OB284	CENBG	3.2	12.6	78.1	4.4	0.46	0.065	0.065	0.79	30	16	198	24	–	78	–
OB291	CENBG	3.2	12.7	78.4	4.8	0.46	0.064	0.067	1.00	26	18	250	27	–	84	–
OB219	CENBG	3.3	12.7	77.9	4.5	0.48	0.059	0.063	0.79	23	16	235	14	–	73	21
OB259	CENBG	3.2	12.7	79.1	4.7	0.49	0.066	0.064	0.82	21	16	207	17	–	68	–
OB224	C2RMF	3.3	12.6	78.2	4.5	0.43	0.058	0.064	0.80	20	16	207	13	22	74	27
OB231	CENBG	3.3	12.8	77.8	4.4	0.49	0.069	0.066	0.78	26	16	259	14	–	70	28
OB235	CENBG	3.3	12.7	79.3	4.7	0.45	0.066	0.057	0.83	22	17	203	14	–	75	–
OB236	CENBG	3.3	12.7	77.8	4.6	0.46	0.053	0.070	0.78	25	14	209	8	–	79	–
OB237	CENBG	3.3	12.8	79.4	4.6	0.43	0.053	0.063	0.77	21	18	239	18	–	71	–
OB263	CENBG	3.3	12.5	77.7	5.0	0.53	0.088	0.081	1.05	31	23	282	21	–	93	–
OB267	CENBG	3.3	12.8	78.2	4.4	0.46	0.067	0.052	0.68	23	14	213	24	–	–	26
OB269	C2RMF	3.3	12.7	78.4	4.8	0.51	0.083	0.072	0.96	29	21	265	23	–	90	–
OB282	CENBG	3.3	12.8	79.2	4.7	0.48	0.064	0.060	0.78	23	16	224	14	–	81	–
OB201	CENBG	3.4	12.9	78.6	4.6	0.48	0.068	0.068	0.84	27	17	213	14	–	73	–
OB249	CENBG	3.4	12.7	78.3	4.8	0.49	0.078	0.071	0.98	26	20	237	21	–	85	–
OB222	CENBG	3.5	12.8	79.0	4.6	0.47	0.063	0.058	0.82	26	18	238	14	–	90	–
OB273	C2RMF	3.5	12.6	77.9	4.5	0.44	0.058	0.060	0.81	20	15	195	16	23	72	24
OB211	CENBG	3.6	12.7	78.0	4.4	0.48	0.057	0.057	0.67	23	14	179	15	–	72	28
OB239	CENBG	3.7	12.8	79.1	4.4	0.44	0.055	0.064	0.81	21	16	209	9	–	81	–
OB260	CENBG	3.7	12.7	77.9	4.3	0.49	0.061	0.063	0.70	20	14	204	8	–	82	29
OB223	CENBG	3.9	12.6	77.6	4.7	0.51	0.068	0.080	1.05	23	22	304	18	–	96	–
OB258	CENBG	4.0	12.6	78.2	4.7	0.50	0.076	0.070	0.91	29	20	274	6	–	95	–
Average		3.1	12.7	78.5	4.6	0.47	0.066	0.065	0.82	24	16	220	16	23	79	25
st. dev.		0.5	0.2	0.5	0.2	0.02	0.010	0.007	0.10	3	2	28	5	3	9	3
var. coef., %		16	1.2	0.7	3.7	5.00	16	11	12	14	14	13	29	14	11	13
Ca–Fe and Sr–Zr rich artefacts																
OB238	CENBG	2.6	13.5	72.4	5.1	1.13	0.213	0.087	1.74	66	21	241	156	–	164	–
OB217	CENBG	3.2	12.8	74.9	5.1	1.27	0.156	0.098	1.72	69	25	258	154	–	171	–
OB243	CENBG	3.2	13.5	73.1	5.1	1.14	0.155	0.084	1.50	52	20	214	139	–	152	–
OB281	CENBG	3.5	13.6	75.4	4.3	1.01	0.133	0.070	1.23	44	16	184	120	–	129	–
OB250	CENBG	3.6	13.6	75.4	4.3	1.05	0.142	0.062	1.19	42	18	193	128	–	136	–
OB251	CENBG	3.6	13.7	75.2	4.3	1.02	0.124	0.068	1.23	42	17	182	128	–	133	–
OB279	CENBG	3.6	13.3	73.6	4.4	1.14	0.158	0.081	1.57	54	20	205	134	–	136	–
OB280	CENBG	3.6	13.7	75.8	4.2	0.96	0.109	0.063	1.14	42	16	178	110	–	129	–
OB287	CENBG	3.6	13.7	75.5	4.2	1.01	0.128	0.063	1.17	41	15	178	113	–	114	–
OB293	CENBG	3.6	13.6	74.3	4.4	1.06	0.136	0.077	1.42	50	18	202	126	–	144	–
OB294	CENBG	3.6	13.7	74.5	4.3	1.06	0.137	0.071	1.36	47	20	203	139	–	134	–
OB276	CENBG	3.7	13.7	75.7	4.3	1.00	0.113	0.062	1.14	42	16	178	120	–	116	–
OB283	CENBG	3.7	13.7	75.1	4.3	1.05	0.133	0.065	1.20	44	14	174	116	–	133	–
OB285	CENBG	3.7	13.7	75.6	4.2	1.01	0.122	0.060	1.15	40	16	161	117	–	143	–
OB286	CENBG	3.7	13.8	75.4	4.2	1.14	0.118	0.062	1.13	42	17	174	120	–	113	–
OB288	CENBG	3.7	13.8	75.6	4.1	0.95	0.124	0.062	1.13	40	16	178	110	–	115	–
OB292	CENBG	3.7	13.8	76.0	4.1	0.99	0.111	0.063	1.10	38	14	169	115	–	117	–
OB295	CENBG	3.7	13.7	75.8	4.1	0.97	0.121	0.064	1.13	41	18	173	118	–	117	–
OB297	CENBG	3.7	13.8	75.6	4.2	1.02	0.126	0.062	1.13	40	17	181	120	–	131	–

(*continued on next page*)

Table 6 (*continued*)

Sample	Facility	Na_2O	Al_2O_3	SiO_2	K_2O	CaO	TiO_2	MnO	Fe_2O_3	Zn	Ga	Rb	Sr	Y	Zr	Nb
OB298	CENBG	3.7	13.7	75.5	4.3	1.02	0.139	0.065	1.15	40	17	175	115	–	123	–
OB271	CENBG	3.8	13.6	74.9	4.3	1.06	0.133	0.072	1.26	50	16	182	122	–	116	–
OB275	CENBG	3.8	13.6	75.4	4.2	1.00	0.121	0.068	1.16	44	17	178	116	–	122	–
OB290	CENBG	3.8	13.7	75.4	4.2	1.02	0.122	0.065	1.17	44	17	178	118	–	125	–
OB274	CENBG	4.0	13.5	74.8	4.3	1.01	0.131	0.070	1.30	46	16	195	126	–	150	–
Average		3.6	13.6	75.0	4.4	1.05	0.134	0.069	1.27	46	17	189	124		132	
st. dev.		0.3	0.2	0.9	0.3	0.07	0.022	0.010	0.19	8	2	23	12		16	
var. coef., %		7.5	1.5	1.2	6.7	6.90	16	14	15	17	14	12	10		12	

Contents in oxides are in weight per cent and contents in elements in μg/g (ppm).

on the basis of the SEM-EDS data, the *likelihood* is that these 43 artifacts were all made from East Göllü Dağ obsidians. It was to resolve the SEM-EDS sourcing uncertainties of the low Ca–Fe obsidians that all these samples were then re-analyzed using other techniques. Of these 43 artifacts, 26 were re-analyzed by EDXRF at UC Berkeley, while 17 were re-run using PIXE, nine at CENBG, six at C2RMF and two on the two facilities (Table 1). We also here took the opportunity to run some of these problem artifacts more than once to undertake a small inter-lab comparison, whereby one piece analyzed at UCB's XRF lab was also run at C2RMF (OB200), while three of those re-analyzed at CENBG were also then re-run at C2RMF (OB220, OB233, OB296).

6. Sourcing by PIXE

Most of the source sample data generated by PIXE were obtained from polished sections, some of which had previously been analyzed by SEM-EDS; the other samples were treated on freshly exposed surfaces (Table 5). In general the contents of fifteen elements were determined except for Y and Nb in an early phase of this work at CENBG, and for Sr which for the Acıgöl Crater sample is always below detection level. The single polished section of samples P35-18B1 (East Göllü Dağ), Al Te 1 (Ala Tepe, Bingöl area) and Orta D2 (Orta Duz, Bingöl area) were analyzed twice, at C2RMF and CENBG respectively. The excellent agreement between the results obtained in these two facilities confirms the equivalence between the extracted beam (C2RMF) and vacuum chamber (CENBG) PIXE declinations for obsidian analyses as previously claimed (Le Bourdonnec et al., 2005). It had also been shown previously that the element contents determined in obsidians by our group using PIXE and ICP-AES/MS were in good agreement, with mean relative standard deviations per element better than 10 per cent to (for Ti) 15 per cent (Bellot-Gurlet et al., 2005, Fig. 4). While this estimation had already been deduced through working with Andean obsidians (Bellot-Gurlet et al., 2008) this is the first time that we can demonstrate that this agreement holds also for the major Anatolian sources (Fig. 7). From Na to Zn and for Zr it is almost always better than 20% and often within 10%. The dispersion is high for Mn due to the fact that PIXE can only obtain this element with limited precision. In Rb and Sr, the PIXE element contents are on the average higher by about 15% and 20% respectively as compared to ICP-MS. The overall distinction between the obsidian sources of Table 5 relies essentially on their Ca, Fe, Zn, Sr and Zr contents and to a lesser extent, to their Al, Si, Ti, Y and Nb contents.

The PIXE data on the Çatalhöyük artifacts are reported in Table 6. Only thirteen element contents were systematically determined in the early phases of this work, to which Y and Nb were then added. In three cases (samples OB 220, 233 and 296) a polished section was analyzed at C2RMF and at CENBG. The agreement inside each data couple is excellent, with the exception of Na, possibly because of a heterogeneously altered surface, as sometimes observed in hydrated obsidians. The five artifacts for which SEM-EDS data were obtained on internal surfaces were also analyzed by PIXE. The agreement between the two methods for the polished surfaces (SEM-EDS) and the archaeological surfaces (PIXE) is excellent for Si, K, Ca and Fe, while Al is always slightly higher in PIXE analyses. The PIXE Na contents are mostly below the expected value for obsidians and do not correspond to their SEM-EDS counterparts. This again argues in favor of non-homogeneously altered archaeological surfaces. The good agreement between PIXE/external surfaces and SEM/internal surfaces for elements Si to Fe is to be related to the larger efficient depth of analysis by PIXE ($\leq$6 μm for Na against $\geq$18 μm for the Si and heavier elements) than for SEM-EDS ($<$4 μm), which tends to be affected to a greater extent by chemically modified surface layer (first micron or so thick) that results from artifact hydration.

As with the SEM-EDS analyses, PIXE provided us with two relatively homogeneous compositional groups of 45 and 24 artifacts based on their Ca and Fe contents respectively (Table 6). They can also be easily distinguished from each other on the basis of their Zn, Sr and Zr contents. In each group the elemental composition is fairly constant, with variation coefficients around the mean values lower than 7% for the Al, Si, K, and Ca oxide contents and lower than 17% for the other elements except Sr in the low Ca–Fe group. The higher dispersion of 29% found for Sr in the low-Ca group is to be related to its 'low' content, being only slightly above detection level. The Na oxides' (see below) large dispersion of 16% and 28% in the low and high Ca–Fe groups respectively is a consequence of surface alteration.

In most cases the contents of Ca, Fe, Zn, Sr and Zr allow us to determine the likely source of the artifacts' raw materials. Thus in binary plots comparing the contents of Sr, Zr and Zn, we view two well-separated artifacts groups, particularly with reference to their Sr contents (Fig. 8). That said, for these and other PIXE-determined trace elements, the high Sr group does not allow us to distinguish between Nenezi Dağ and Orta-Sakaeli source compositions. However, as documented in Table 5 the latter can be discriminated on the basis of their major element Ca and Fe contents. In turn we exclude Kocadağ as a possible source for the Çatalhöyük obsidian on the basis of the artifacts' Zr, Sr and Fe values as the Zr and Sr contents are always higher and lower respectively for this source compared to Nenezi Dağ obsidians (Table 5; see also Keller and Seifried, 1990). Furthermore, as detailed above, among the major elements, the Fe contents are always lower than in Nenezi Dağ obsidians.

With the 'low Sr' artifact group in Fig. 8, Sr is close to the Göllü Dağ and Süphan Dağ source compositions. The separation of the artifact group from a WGD composition on the basis of their higher Sr contents, is also confirmed by the slightly higher Ca content of this source compared to EGD obsidians (as previously observed by other archaeometrists [Keller and Seifried, 1990; Poidevin, 1998 and Table 2 here]). With regard to the Süphan Dağ source composition, the Çatalhöyük samples systematically show Zn

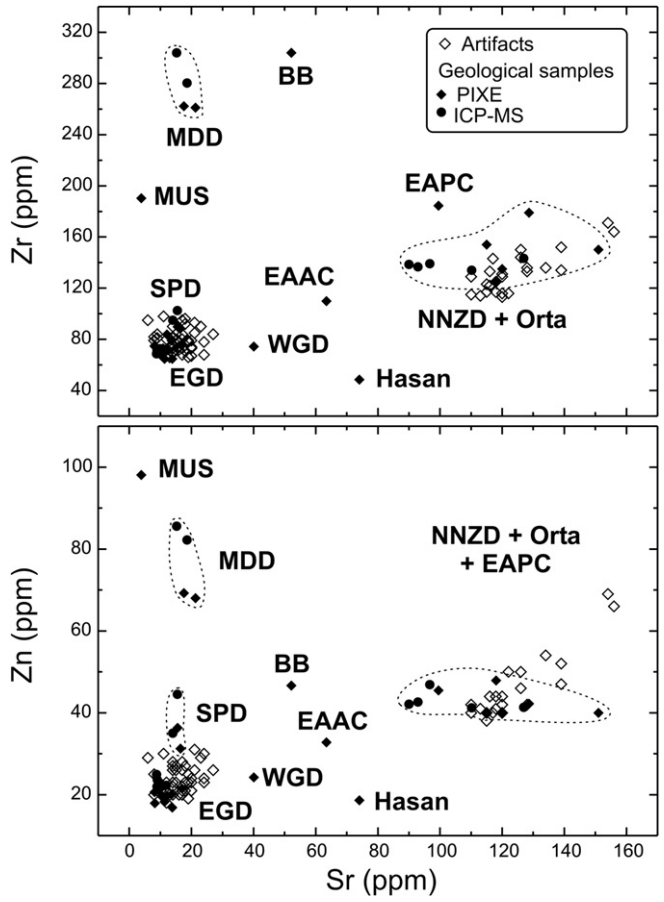

Fig. 8. Comparison between the contents of Sr, Zn and Zr in the Çatalhöyük artifacts and in obsidians from potential sources as determined by PIXE.

contents subtly lower than the two geological samples analyzed, but also significantly different Ca and Fe contents which suggest that we can exclude this volcanic centre as a potential source of our artifacts' raw material. The Ca and Fe contents thus also serve to discriminate the artifacts' raw material from those of Süphan Dağ and WGD.

In summary, while SEM-EDS could not differentiate between East Göllü Dağ and West Acıgöl with regard to the source of the 45 low-Ca obsidians from Çatalhöyük, PIXE allows us to assign with confidence the group to East Göllü Dağ, largely on the basis of their Sr contents. With regard to the 25 high-Ca artifacts, the SEM-EDS and PIXE data converge towards indicating a Nenezi Dağ compositional type.

7. Sourcing by EDXRF

At UC Berkeley's XRF lab we analyzed 34 artifacts and four geological samples. The latter comprised Or4 and Sa1 from Galatia plus N8 from the Acıgöl Crater which had also been analyzed by PIXE, while Kom-1 from the Kömürcü source (East Göllü Dağ) had previously been run by ICP-MS. In all cases the agreement between EDXRF and the other two approaches was excellent for all elements. The Ba content, although in the range admitted for an East Göllü Dağ sample is higher by more than 40% than in the aliquot of sample Kom-1 also analyzed by ICP-MS.

The 34 artifacts can again, as with PIXE, be separated into two low and high Sr–Zr groups respectively. While these groups present similar contents in Mn, Rb, Y, Nb and Th, they differ also greatly by their respective low and high Ba contents (Table 7).

Table 7
Elemental compositions of Çatalhöyük obsidian artifacts as determined by EDXRF.

Sample	MnO[a]	Ga	Rb	Sr	Y	Zr	Nb	Ba	Pb	Th
Sr–Zr poor artifacts										
200	0.06	16	196	13	29	82	26	128		28
202	0.06	17	211	10	22	85	22	131		29
204	0.06	17	199	12	24	77	20	116		23
207	0.06	16	207	16	26	80	22	151		27
210	0.07	19	211	15	26	82	23	130		32
211	0.06		190	21	23	87	22	223		24
214	0.06	17	208	13	26	79	24	118		33
216	0.07	18	215	13	25	83	26	155		24
218	0.06	18	195	13	27	80	21	116		25
225	0.07	19	206	18	28	86	26	246		30
227	0.07	19	209	13	28	81	27	125		29
232	0.06	16	187	10	23	75	19	125		27
240	0.06	17	192	17	25	79	22	224		30
241	0.05	16	188	11	23	82	23	145		38
244	0.08	20	222	18	26	90	27	221		24
245	0.06	15	190	13	23	74	23	138		22
246	0.05	15	175	11	24	74	26	132		30
247	0.07	17	210	10	24	81	21	143		29
248	0.06	18	198	11	24	78	22	121		28
252	0.06	18	203	13	25	81	23	144		31
261	0.06	17	198	11	25	85	27	152		27
262	0.06	18	192	14	22	83	22	199		32
264	0.05	17	181	15	24	78	24	206		20
265	0.06	15	187	11	25	81	20	226		28
270	0.060	18	182	17	23	79	23	201		27
273	0.056		191	18	26	92	23	169		17
Average	0.061	17	198	14	25	81	23	161		27
st. dev.	0.006	1	12	3	2	4	2	42		4
var. coef., %	9.446	8	6	22	7	5	10	26		16
Sr–Zr rich artifacts										
212	0.064		172	98	22	146	22	875	30	34
213	0.067		169	101	23	143	19	840	33	31
215	0.063		170	100	23	145	17	756	30	31
228	0.062		168	95	21	138	17	843	26	30
256	0.075		183	103	19	159	19	920	32	31
272	0.065		167	96	24	146	17	802	32	34
277	0.086		170	96	20	143	18	853	36	39
278	0.062		204	115	22	158	20	856	31	44
Average	0.068		175	101	22	147	19	843	31	34
st. dev.	0.008		13	6	2	7	2	49	3	5
var. coef., %	12		7	6	8	5	9	6	9	14

[a] Element contents in weight per cent oxide for Mn and in μg/g for the others.

In the high Sr–Zr group, as for PIXE, a Sr–Zr diagram cannot separate a Nenezi Dağ from a Galatian origin (Fig. 9). However the latter is easily eliminated from its larger Th contents (>20 ppm) than in the former (<8 ppm) (Table 5). With regard to Ba, the high contents above 800 ppm found by EDXRF in these artifacts are unknown in Cappadocia and Galatia, where they reach at most 560 ppm except at Hasan Dağ (Poidevin, 1998). However, if in this source the Ba contents are in the range 750–1000 ppm, the Sr contents are lower than in the Nenezi Dağ obsidians (Poidevin, 1998) and in the Çatalhöyük high Sr–Zr and Ca–Fe obsidians. This suggests that the barium might also be somewhat overestimated by EDXRF (see also KOM-1 in Table 5).

In the low Sr–Zr group, while the Çatalhöyük artifacts match the EGD type composition, they also lay side-by-side with the West Acıgöl and Süphan Dağ obsidians. A WA origin for this material can easily be rejected on the ground of their lower Sr (<4 ppm in Table 4) and especially Ba (29 ppm) values as compared to EGD obsidians (Poidevin, 1998; Bellot-Gurlet, 1998 *inter alia*). The only WA sample analyzed by EDXRF also presents slightly higher contents in Rb, Y and marginally in Ga than the EGD obsidians. In turn, the low content of Ba (<210 ppm) in the group of low Sr–Zr artifacts is sufficient to eliminate the Süphan Dağ source (<478 in Table 5), as is possibly the Nb content.

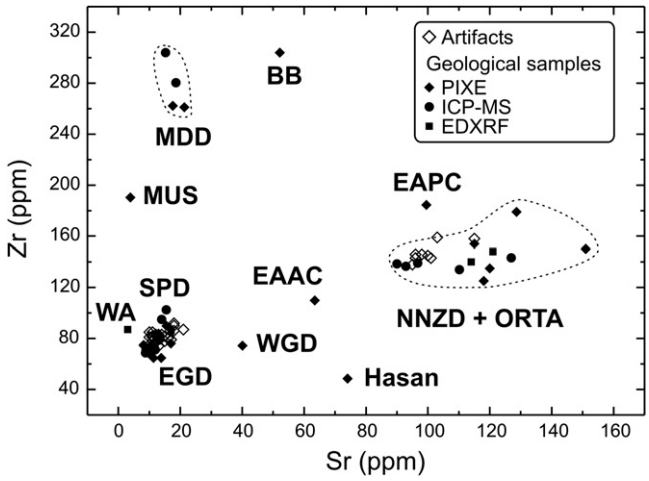

Fig. 9. Comparison between the contents of Sr and Zr in the Çatalhöyük artifacts and in obsidians from potential sources as determined by EDXRF.

Thus in spite of having determined the elemental composition of only four source samples, the technique appears capable of sourcing the low Sr–Zr Çatalhöyük obsidians to East Göllü Dağ and the high Sr–Zr group to the Nenezi Dağ.

8. Summary and conclusion

The past forty years of obsidian sourcing in the Near and Middle East have largely been based upon characterizing the material through reference to its chemical composition, primarily at the trace elemental level. The possibility of achieving the same end by using only major elements contents using partially destructive SEM-EDS was suggested nearly twenty years ago by Keller and Seifried (1990), albeit in a study that only involved the analysis of 14 artifacts from four Anatolian sites. The second study to use this technique in a Near Eastern context involved a significantly larger data set, with the recent analysis of 136 artifacts from the Final Natufian site of Ain Mallaha (Eynan) in Israel (Delerue and Poupeau, 2007, p. 291–296). The methods used in this study – undertaken by two of the current authors – are the same as those detailed above in Section 4. While the only two artifacts from Ain Mallaha analyzed from polished sections generated a typical EGD/WA composition, the 134 other samples that were treated non-destructively produced a spectrum of elemental compositions similar to those observed for the Çatalhöyük artifacts (detailed above), with an even larger dispersion in Na_2O contents, from 1.18% to 4.32% (Delerue and Poupeau, 2007). However, taking into consideration their overall elemental composition and the fact that during the Natufian only East Göllü Dağ obsidians are known to have reached the Levant (Chataigner, 1998; Delerue, 2007) the interpretation was forwarded that the raw material of the Ain Mallaha artifacts was from EGD rather than WA (Delerue and Poupeau, 2007). These data further indicate that the alteration processes affecting the near-surface elemental composition of the obsidian from Çatalhöyük seems to be a general taphonomic process affecting all buried artifacts, as opposed to a site-specific (Konya Plain) phenomenon. Therefore, while SEM-EDS has been shown that it *can* make a contribution to the discrimination of archaeologically significant obsidian sources through a non-destructive analysis of their major element contents, we would recommend working on polished sections in order to limit ambiguities in source assignation. That said, the technique remains incapable of distinguishing between the two Cappadocian sources of East Göllü Dağ and West Acıgöl. This limitation is clearly overcome by EDXRF, which has the advantage of being non-destructive. The eight elements determined here can discriminate between Nenezi Dağ and Galatia obsidians. EDXRF therefore offers a rich potential for future Near Eastern obsidian studies (see also Kobayashi et al., 2003; Mochizuki, 1997). Finally, we are confident that these analyses demonstrate that PIXE is a technique capable of unambiguously sourcing obsidians in an Anatolian/Near Eastern context (see also Abbès et al., 2003), alongside such established but partially destructive methods as ICP-MS/-AES, LA-ICP-MS, NAA and Fission Track Dating (Gomez et al., 1995; Bigazzi et al., 1998; Gratuze, 1999; Abbès et al., 2003; Carter et al., 2006 *inter alia*). While this research group's work represents the first applications of this method in an East Mediterranean context, it should be noted that PIXE has already been successfully employed for the sourcing of archaeological obsidians in Australasian, Mesoamerican, South American, Transylvanian and West Mediterranean contexts (Summerhayes et al., 1998; Bellot-Gurlet et al., 1999; Constantinescu et al., 2002; Lugliè et al., 2007; Rivero-Torres et al., 2008).

The 100 Çatalhöyük artifacts analyzed in this study were all shown to be made of southern Cappadocian obsidians, the majority associated with the East Göllü Dağ compositional group ($n = 68$), the remainder having a chemical signature that matched that of the Nenezi Dağ source ($n = 32$). The fact that these artifacts were made of obsidian from these two sources comes as no great surprise given that previous analyses had clearly indicated these to be the preferred raw materials not only for the inhabitants of Çatalhöyük (Carter et al., 2006; Carter and Shackley, 2007), but also prehistoric communities throughout central Anatolia, Cyprus and the Levant more generally (Chataigner, 1998, 285–292). That, of course, is not the end of the story as the new data indicates significant differences with regard to how these obsidians were being consumed at Çatalhöyük, with the East Göllü Dağ products clearly the primary raw material used during the Aceramic Neolithic (Level Pre-XII) and the first half of the Early Pottery Neolithic, up to c. Level VIB, with a radical shift thereafter towards the use of Nenezi Dağ obsidian in conjunction together with a major change in technology (see also Carter et al., 2006). The archaeological implications of these new data will discussed more fully elsewhere by Carter and Milić.

To conclude, our study shows that PIXE, EDXRF, and to a certain extent SEM-EDS, constitute powerful approaches for obsidian characterization studies in an Anatolian/Near Eastern context, not least due to their representing non-destructive alternatives, an extremely important consideration for archaeologists, archaeometrists and local museum custodians alike.

Acknowledgements

The authors wish to thank Floréal Daniel and Yannick Lefrais for their efficient management of the CRP2A scanning electron microscope and Ludovic Bellot-Gurlet (LADIR, Thiais), Giulio Bigazzi (Istituto di Geoscienze e Georesorce, Pisa), Marie-Claire Cauvin (Institut de Préhistoire Orientale, Jalès) and Jean-Louis Poidevin (Université de Clermont-Ferrand) for having provided them obsidian source samples. We further acknowledge the long-term support of Ian Hodder, Shahina Farid and our representatives from the Konya Museum and the Turkish Ministry of Culture. Carter's time at CRP2A was funded by an Initiative Award from the France-Stanford Center for Interdisciplinary Studies, Stanford University (2007) and a grant from the Scientific Service, French Embassy in Canada (2008). EDXRF analyses by Shackley at Berkeley were funded, in part, by a United States National Science Foundation grant (BCS-0716333).

Appendix 1. Geological samples localization.

Area	Sample	Sampling station, when specified	Provided by
Orta-dome	Or 4		Poidevin
Sakaeli-dome	Sa 1	17 km north of Orta, edge of a dome	Poidevin
Acigöl crater	N8	Acigöl, wall of maar, 2 km E of Aciğöl, S of Acigöl-Nevsehir road	Bigazzi*
Kocadağ	N4	Taskesiktepe, 700 m W of Bogazköy	Bigazzi*
WTHD	N1	Boğazköy (wall of caldera 1 km NNW of Boğazköy, N of Acigöl-Nevsehir road	Bigazzi*
East Kayırlı	P35-18B1	W flank of Bitlikeler hill	Cauvin
	Kay E1		Poidevin
Kömürcü	Kom 1		Poidevin
	Kom C1 to C6	Gully along the Komürcü 'C flow'	Cauvin
Sirça Deresi	SD1 and SD2	Not specified	Carter
North-Bozköy	N12	1 km E of Bozköy or 1 km E of Komürcü	Bigazzi*
Nenezi Dağ	P34.8	Nenezi Dağ west gully	Cauvin
	Ne W2 and NE 5		Poidevin
Hasan Dag	Hasan and Has-Kay		Bigazzi
Ala Tepe	Al Te 1		Cauvin
Orta Duz	Orta D1 and D2		Cauvin
	BIN 9-1	Karan village (Karan Solhan area), between Bingöl and Mus	Kobayashi
Meydan Dağ	ME 6-1	Outside caldera	Kobayashi
	ME 7-1	Inside caldera (Obsidian source No. 6 in Kobayashi et al., 2003)	Kobayashi
	Mey 1 and Mey 4		Poidevin
Mus	D20	Mercimekkale, near to Anzar	Bigazzi**
	MUS-Ziy	Mus-Ziyaret Tepe	Bigazzi
Nemrut Dağ	Nem N1 and N2	Northern part of Nemrut Dağ	Poidevin
	NEM 3-1	Sampling site 3 is a secondary source inside the caldera (Obsidian source No. 8)	Kobayashi***
	NEM 3-2		
	NEM 3-3		
Suphan Dağ	Sup 1	SW of Suphan Dağ	Poidevin
	Sup 5	NE of Suphan Dağ	Poidevin
	SU 5-1	Obsidian source No. 7 in Kobayashi et al. (2003)	Kobayashi

*Bigazzi et al. (1993); **Bigazzi et al. (1994); ***Kobayashi et al. (2003). All others, pers. com.

References

Abbès, F., Bellot-Gurlet, L., Cauvin, M.-C., Delerue, S., Dubernet, S., Poupeau, G., Stordeur, D., 2003. Provenance of the Jerf el Ahmar (Middle Euphrates Valley, Syria) obsidians. Journal of Non-Crystalline Solids 323, 162–166.

Adams, P.B., 1984. Glass corrosion. Journal of Non-Crystalline Solids 67, 193.

Anowitz, L.M., Elam, J.M., Riciputi, L.R., Cole, D.R., 1999. The failure of obsidian hydration dating: sources, implications, and new directions. Journal of Archaeological Science 26, 735–752.

Balkan-Atli, N., Der Aprahamian, G., 1998. Les nucléus de Kaletepe et deux ateliers de taille en Cappadoce. In: Cauvin, M.-C., Gourgaud, A., Gratuze, B., Arnaud, N., Poupeau, G., Poidevin, J.-L., Chataigner, C. (Eds.), L'Obsidienne au Proche et Moyen Orient. Du volcan à l'outil. BAR International Series 738. Archaeopress, Oxford, pp. 241–258.

Balkan-Atli, N., Cauvin, M.-C., Binder, D., 1999. Obsidian: sources, workshops and trade in Central Anatolia. In: Özdoğan, M., Başgelen, N. (Eds.), Neolithic in Turkey: The Cradle of Civilization. New Discoveries. Arkeoloji ve Sanat Yayınları, Istanbul, pp. 133–145.

Bellot-Gurlet, L., 1998. Caractérisation par analyse élémentaire (PIXE et ICP-MS/-AES) d'un verre naturel:l'obsidienne. Application à l'étude de provenance d'objets archéologiques. Université Joseph Fourier, Grenoble I. http://tel.archives-ouvertes.fr/tel-00315287/fr/.

Bellot-Gurlet, L., Calligaro, Th., Dorighel, O., Dran, J.-C., Poupeau, G., Salomon, J., 1999. PIXE analysis and fission track dating of obsidian from South American prehispanic cultures (Colombia, Ecuador). Nuclear Instruments and Methods in Physics Research Section B 150, 616–621.

Bellot-Gurlet, L., Poupeau, G., Bressy, C., 2003. Element contents determined by ICP-AES and ICP-MS at Grenoble on nine obsidian artefacts from Tell Kosak Shamali: results and inferences on provenance. In: Nishiaki, Y., Matsutani, T (Eds.), Tell Kosak Shamali, vol. 2. The University of Tokyo, pp. 113–119.

Bellot-Gurlet, L., Poupeau, G., Salomon, J., Calligaro, Th., Moignard, B., Barrat, J.A., Pichon, L., 2005. Obsidian provenance studies in archaeology: a comparison between PIXE and ICP. Nuclear Instruments and Methods in Physics Research Section B 240, 583–588.

Bellot-Gurlet, L., Dorighel, O., Poupeau, G., 2008. Obsidian provenance studies in Colombia and Ecuador: obsidian sources revisited. Journal of Archaeological Science 35, 272–289.

Bigazzi, G., Yeğingil, Z., Ercan, T., Oddone, M., Özdoğan, M., 1993. Fission track dating in central and northern Anatolia. Bulletin of Volcanology 55, 588–595.

Bigazzi, G., Yeğingil, Z., Ercan, T., Oddone, M., Özdoğan, M., 1994. Provenance studies of prehistoric artifacts in eastern Anatolia: interdisciplinary research results. Mineralogica et Petrographica Acta XXXVII, 17–36.

Bigazzi, G., Poupeau, G., Yeğingil, Z., Bellot-Gurlet, L., 1998. Provenance studies of obsidian artefacts in Anatolia using the fission-track dating method: an overview. In: Cauvin, M.-C., Gourgaud, A., Gratuze, B., Arnaud, N., Poupeau, G., Poidevin, J.-L., Chataigner, C. (Eds.), L'Obsidienne au Proche et Moyen Orient. Du volcan à l'outil. BAR International Series 738. Archaeopress, Oxford, pp. 69–89.

Binder, D., Balkan-Atli, N., 2001. Obsidian exploitation and blade technology at Kömürcü-Kaletepe (Cappadocia, Turkey). In: Caneva, I., Lemorini, C., Zampetti, D., Biagi, P. (Eds.), Beyond Tools. Redefining the PPN Lithic Assemblages of the Levant. Proceedings of the Third Workshop on PPN Chipped Lithic Industries. Studies in Early Near Eastern Production, Subsistence, and Environment, vol. 9. Ex Oriente, Berlin, pp. 1–16.

Bressy, C., Poupeau, G., Yener, A., 2005. Cultural interactions during the Ubaid and Halaf periods: Tell Kurdu (Amuq Valley, Turkey) obsidian sourcing. Journal of Archaeological Science 32, 1560–1565.

Calligaro, T., MacArthur, J.D., Salomon, J., 1996. An improved experimental setup for the simultaneous PIXE analysis of heavy and light elements with a 3 Mev proton external beam. Nuclear Instruments and Methods in Physics Research Section B 109/110, 125–128.

Calligaro, T., Dran, J.-C., Moignard, B., Pichon, L., Salomon, J., Walter, P., 2002. Ion beam analysis with external beams: recent set-up improvements. Nuclear Instruments and Methods in Physics Research Section B 188, 135–140.

Calligaro, T., Dran, J.-C., Poupeau, G., Gendron, F., Dubernet, S., Meslay, O., Gonthier, E., Tenorio, D., 2005. PIXE reveals that two Murillo's masterpieces were painted on Mexican obsidian slabs. Nuclear Instruments and Methods in Physics Research B 240, 576–582.

Campbell, J.L., Hopman, T.L., Maxwell, J.A., Nejedly, Z., 2000. The Guelph PIXE software package III: alternative proton database. Nuclear Instruments and Methods in Physics Research Section B 170, 193–204.

Carter, T., Shackley, M.S., 2007. Sourcing obsidian from Neolithic Çatalhöyük (Turkey) using energy dispersive x-ray fluorescence. Archaeometry 49, 437–454.

Carter, T., Poupeau, G., Bressy, C., Pearce, N.J.G., 2005a. From chemistry to consumption: towards a history of obsidian use at Çatalhöyük through a programme of inter-laboratory trace elemental characterization. In: Hodder, I. (Ed.), Changing Materialities at Çatalhöyük: Reports from the 1995–1999 Seasons. Mc Donald Institute Monographs and BIAA, Cambridge, pp. 285–305. 535–557.

Carter, T., Conolly, J., Spasojević, A., 2005b. The chipped stone. In: Hodder, I. (Ed.), Changing Materialities at Çatalhöyük: Reports from the 1995–1999 Seasons. McDonald Institute Monographs and BIAA, Cambridge, pp. 221–283. 467–533.

Carter, T., Poupeau, G., Bressy, C., Pearce, N.J.G., 2006. A new programme of obsidian characterization at Çatalhöyük, Turkey. Journal of Archaeological Science 33, 893–909.

Carter, T., Dubernet, S., King, R., Le Bourdonnec, F.-X., Milić, M., Poupeau, G., Shackley, M.S., 2008. Eastern Anatolian obsidians at Çatalhöyük and the reconfiguration of regional interaction in the Early Pottery Neolithic. Antiquity 82, 900–909.

Cauvin, M.-C., Balkan-Atli, N., 1996. Rapport sur les recherches sur l'obsidienne en Cappadoce, 1993–1995. Anatolia Antiqua IV, 249–271.
Cessford, C., Blumbach, P., Göze Akoğlu, K., Higham, T., Kuniholm, P.I., Manning, S.W., Newton, N.W., Özbakan, M., Melek Özer, A., 2005. Absolute dating at Çatalhöyük. In: Hodder, I. (Ed.), Changing Materialities at Çatalhöyük: Reports from the 1995–1999 Seasons. McDonald Institute Monographs and BIAA, Cambridge, pp. 65–99. 449–450.
Chabot, J., Poidevin, J.-L., Chataigner, C., Fortin, M., 2001. Caractérisation et provenance des artefacts en obsidienne de Tell 'Atij et de Tell Gudeda (III^{e} millénaire, Syrie). In: Fortin, M. (Ed.), Recherches canadiennes sur la Syrie antique / Canadian Research on Ancient Syria. Musée de la civilisation. Canadian Society for Mesopotamian Studies. Québec, Toronto, pp. 241–256.
Chataigner, C., 1998. Sources des artefacts du Proche Orient d'après leur caractérisation géochimique. In: Cauvin, M.-C., Gourgaud, A., Gratuze, B., Arnaud, N., Poupeau, G., Poidevin, J.-L., Chataigner, C. (Eds.), L'Obsidienne au Proche et Moyen Orient. Du volcan à l'outil. BAR International Series 738. Archaeopress, Oxford, pp. 273–324.
Constantinescu, B., Bugoi, R., Sziki, G., 2002. Obsidian provenance studies of Transylvania's Neolithic tools using PIXE, micro-PIXE and XRF. Nuclear Instruments and Methods in Physics Research Section B 189, 373–377.
Davis, M.K., Jackson, T.L., Shackley, M.S., Teague, T., Hampel, J.H., 1998. Factors affecting the energy-dispersive x-ray fluorescence (EDXRF) analysis of archaeological obsidian. In: Shackley, M.S. (Ed.), Archaeological Obsidian Studies: Method and Theory. Advances in Archaeological and Museum Science, vol. 3. Plenum Press, New York, pp. 159–180.
Delerue, S., 2007. L'obsidienne dans le processus de néolithisation du Proche-Orient (12000–6500 BC). Ph.D., Université Michel de Montaigne, Bordeaux 3.
Delerue, S., Poupeau, G.., 2007. La provenance des obsidiennes du Natoufien final de Mallaha, in Valla, F.R. et al., Les fouilles de Ain Mallaha (Eynan) de 2003 à 2005: Quatrième rapport préliminaire. Journal of the Israel Prehistoric Society vol. 37, 135–379 (291–296).
Ercan, T., Yeğingil, Z., Bigazzi, G., 1989. Obsidian, definition, characteristics and distribution in Anatolia; geochemical features of Central Anatolian obsidians. Jeomorfoloji Dergisi 17, 71–83.
Gale, N.H., 1981. Mediterranean obsidian source characterisation by strontium isotope analysis. Archaeometry 23, 41–51.
Govindaraju, K., 1994. Compilation of working values and sample description for 383 geostandards. Geostandards Newsletter 18, 1994. Special Issue.
Gomez, B., Glascock, M.D., Blackman, J., Todd, I.A., 1995. Neutron activation analysis of obsidian from Kalavasos-Tenta. Journal of Field Archaeology 22, 503–508.
Gratuze, B., 1999. Obsidian characterization by Laser Ablation ICP-MS and its application to prehistoric trade in the Mediterranean and the Near East: sources and distribution of obsidian with the Aegean and Anatolia. Journal of Archaeological Science 26, 869–881.
Hodder, I. (Ed.), 2007. Excavating Çatalhöyük: South, North and KOPAL Area Reports from the 1995–1999 Seasons. McDonald Institute Monographs, Cambridge.
Keller, J., Seifried, C., 1990. The present status of obsidian source identification in Anatolia and the Near East. PACT 25, 57–85.
Kobayashi, K., Zahidul, A.M., Mochizuki, A., 2003. Classification of obsidian sources in Turkey (II). Classification of obsidian sources in Eastern Anatolia. Anatolian Archaeological Studies XII, 109–112.
Le Bourdonnec, F.-X., 2007. Aspects archéométriques de la circulation de l'obsidienne préhistorique. Développements analytiques et applications en Corse, Sardaigne et Ethiopie. Ph. D., Université Michel de Montaigne Bordeaux 3.
Le Bourdonnec, F.-X., Delerue, S., Dubernet, S., Moretto, P., Calligaro, T., Dran, J.C., Poupeau, G., 2005. PIXE characterization of Western Mediterranean and Anatolian obsidians and Neolithic provenance studies. Nuclear Instruments and Methods in Physics Research Section B240, 595–599.
Le Bourdonnec, F.-X., Bontempi, J.-M., Marini, N., Mazet, S., Neuville, P.F., Poupeau, G., Sicurani, J., 2010. Western Mediterranean obsidians characterization by SEM-EDS and the Neolithic site of A Fuata (Corsica). Journal of Archaeological Science 37, 92–106.
Llabador, Y., Bertault, D., Gouillaud, J.C., Moretto, P., 1990. Advantages of high speed scanning for microprobe analysis of biological samples. Nuclear Instruments and Methods in Physics Research Section B 49, 435–440.
Lugliè, C., Le Bourdonnec, F.-X., Poupeau, G., Atzeni, E., Dubernet, S., Moretto, P., Serani, L., 2007. Early Neolithic obsidians in Sardinia (western Mediterranean): the Su Carroppu case. Journal of Archaeological Science 34, 428–439.
Maxwell, J.A., Campbell, J.L., Teesdale, W.J., 1989. The Guelph PIXE software package. Nuclear Instruments and Methods in Physics Research Section B 43, 218–230.
Mellaart, J., 1967. Çatal Hüyük, a Neolithic Town in Anatolia. Thames and Hudson, London.
Mochizuki, A., 1997. Classification of obsidian sources in Turkey (I). Classification of obsidian sources in Central Anatolia and source identification of obsidian artifacts from Kaman-Kalehöyük. Anatolian Archaeological Studies VI, 169–186 (in Japanese).
Patel, S.B., Hedge, R.E., Kilner, J.A., 1998. Surface analysis of archaeological obsidians by SIMS. Journal of Archaeological Science 25, 1047–1054.
Poidevin, J.-L., 1998. Les gisements d'obsidienne de Turquie et de Transcaucasie: géologie, géochimie et chronométrie. In: Cauvin, M.-C., Gourgaud, A., Gratuze, B., Arnaud, N., Poupeau, G., Poidevin, J.-L., Chataigner, C. (Eds.), L'Obsidienne au Proche et Moyen Orient. Du volcan à l'outil. BAR International Series 738. Archaeopress, Oxford, pp. 105–203.
Rivero-Torres, S., Calligaro, Th., Tenorio, D., Jiménez-Reyes, M., 2008. Characterization of archaeological obsidians from Lagartero, Chiapas Mexico by PIXE. Journal of Archaeological Science 35, 3168–3171.
Renfrew, C., Dixon, J.E., Cann, J.R., 1966. Obsidian and early Cultural Contact in the near East. Proceedings of the Prehistoric Society 22, 30–72.
Shackley, M.S., 2005. Obsidian: Geology and Archaeology in the North American Southwest. University of Arizona Press, Tucson.
Summerhayes, G.R., Bird, J.R., Fullager, R., Gosden, C., Specht, J., Torrence, R., 1998. Application of PIXE-PIGME to archaeological analysis of changing patterns of obsidian use in West New Britain, Papua New Guinea. In: Shackley, M.S. (Ed.), Archaeological Obsidian Studies: Method and Theory. Advances in Archaeological and Museum Science 3. Plenum Press, New York, pp. 129–158.
Wright, G.A., 1969. Obsidian analyses and prehistoric near eastern trade: 7500 to 3500 BC. In: Anthropological Papers, No 37. Museum of Anthropology, University of Michigan, Ann Arbor, pp. 5–26.